Submembrane cytoskeleton-regulated assembly and functional activity of gap junctions

Dissertation

zur Erlangung des Doktorgrades

der Mathematisch-Naturwissenschaftlichen Fakultäten

der Georg-August-Universität zu Göttingen

vorgelegt von

Eugenia Butkevich

aus Omsk, Rußland

Göttingen, 2004

D7

Referent: Prof. Dr. F.-W. Schürmann.

Korreferent: Prof. Dr. R. Jahn

Tag der mündlichen Prüfung: 29.06.2004

Abbreviations

AD	Alzheimer's disease
ATP	adenosine triphosphate
BSA	bovin serum albumine
cAMP	cyclic adenosine monophosphate
Cx	connexin
CT	COOH-terminus
CY-3	indigocarbocyanine
DMEM	Dulbecco's minimal essential medium
DMSO	dimetyl sulfonyl fluorid
E.coli	*Escherichia coli*
EDTA	ethylenediaminetetraacetic acid
EGTA	ethylene glycol-bis(ß-amino-ethyl ether)
ER	endoplasmic reticulum
FCS	foetal calf serum
FRET	fluorescence resonance energy transfer
GJ	gap junction
GST	glutathione S-transferase
GSSG	glutathione (oxidised)
IPTG	isopropyl-thio-ß-D-galactoside
MALDI-Q-TOF MS	matrix assisted laser desorption/ionisation quadripole time of flight mass spectrometry
PAGE	polyacrylamide gel electrophoresis
PM	plasma membrane
PVDV	polyvinylidene difluoride
RT	room temperature
SDS	sodium dodecyl sulfate
si-RNA	small interferens RNA
TEMED	1,2-Bis-(dimethylamino)-ethane
wt	wild type

Contents

1. Introduction

1.1 Preface

Cells communicate with each other in a variety of ways. One way of communication involves gap junctions, which allow for the intercellular transmission of molecules through specialised channels localised to the plasma membrane domains of cell-cell contact (Kumar and Gilula, 1992).

The existence of gap junctions allows an intercellular exchange of low molecular weight molecules including ions, metabolites, and second messengers like cAMP, calcium, and inositol 1,4,5-trisphosphate, but prevents the movement of molecules larger than 1 kDa such as proteins and nucleic acids. Gap junctions provide a pathway linking the cytoplasm of attached cells and contribute to the integration of metabolic activities by setting up networks of communicative cell assemblies. By electrically coupled neurons, gap junctions allow action potential to spread between cells. Key features of electrical transmission are that it is extremely rapid, it is a high fidelity (signals are transmitted with no distortion), and it works in both directions.

Gap junctions are implicated in diverse biological processes, such as development, cellular metabolism, and cellular growth control. Intercellular communications via gap junctions contribute to metabolic co-operation and synchronisation of cellular physiological activities. Electrical coupling allows the rapid and synchronous propagation of action potential in excitable tissues. In the heart gap junctions allow current flows from the pacemaker cells to ventricular muscle cells leading to their synchronised rhythmic contraction. The exchange of second messengers allows the transfer of information between coupled cells. Metabolic coupling is particularly important in the case of non-vascularised tissues, such as the eye lens.

1.2 The connexin family

Gap junctions appeared during the evolutionary appearance of multicellular organisms. Innexins form gap junctions in invertebrates. Although their gene structure is very different from that of connexins, which form gap junctions in vertebrates, they exhibit remarkably similar channel properties (Phelan at al., 2001).

The multigene family of connexins has been divided into three types: α, β and γ or δ (Fig.1) (Gimlich et al., 1990; Kumar and Gilula, 1992, Sohl et al., 1998; Manthey et al., 1999).

Compared with the β type connexins, the α type connexins have a larger M2–M3 cytoplasmic loop and a larger cytoplasmic COOH-terminal tail (see Fig.3).
An alternative nomenclature uses the molecular weight to specify individual connexins (Beyer et al., 1990).
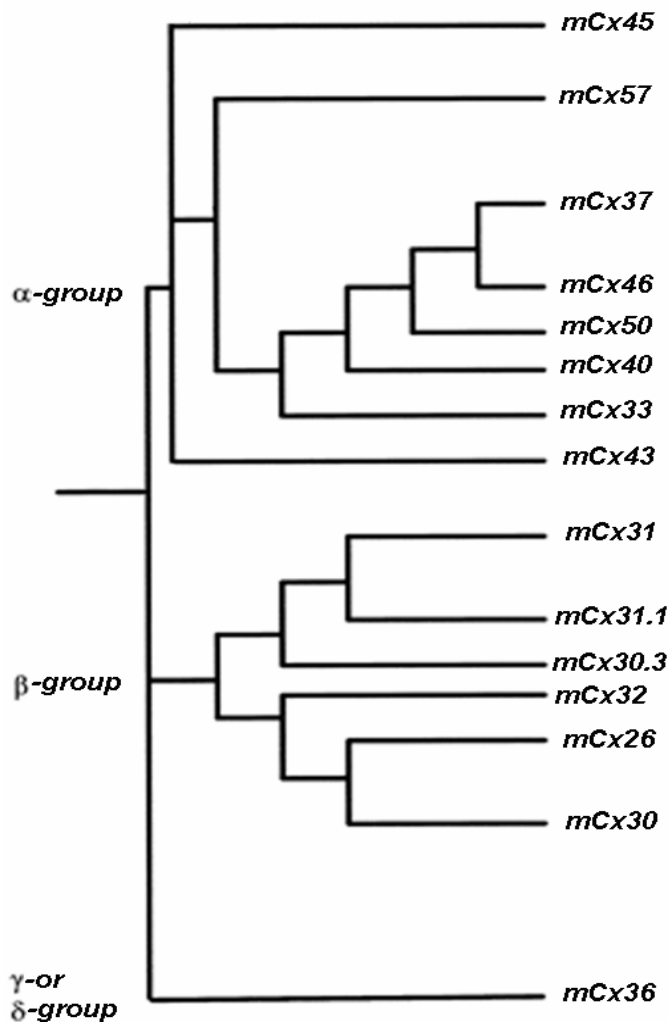
Fig.1 Phylogenetic tree of murine connexins. Taken from D. Manthey et al., JBC, 1999.

1.3 Transmembrane topology of connexins

Docking of two hemichannels of adjacent cells forms gap junction. Each hemichannel (connexon) is composed of six subunits, called connexins (Cx) (Fig.2). Each connexin protein comprises four transmembrane, two extracellular and three cytoplasmic domains (Fig.3). The N- and C-termini of connexins are exposed into the cytoplasm. Major differences in sequence and length were found in the carboxyl terminal region and the cytoplasmic loop of connexins.
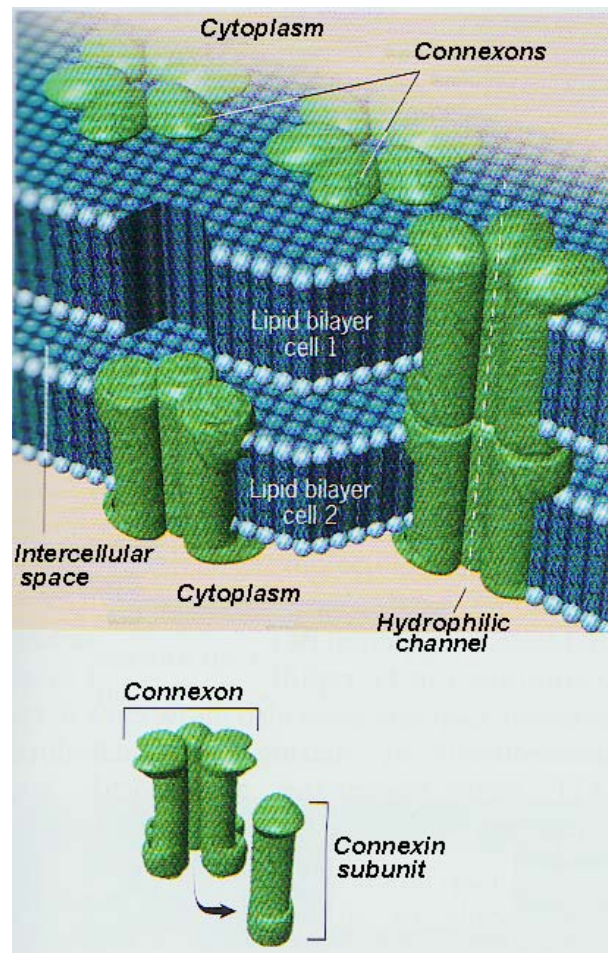
Fig.2 Schematic model of a gap junction channel. The gap junction channel consists of two hemichannels (connexons). Each connexon is composed of six protein subunits, called connexins. Taken from G.Karp, 1999.
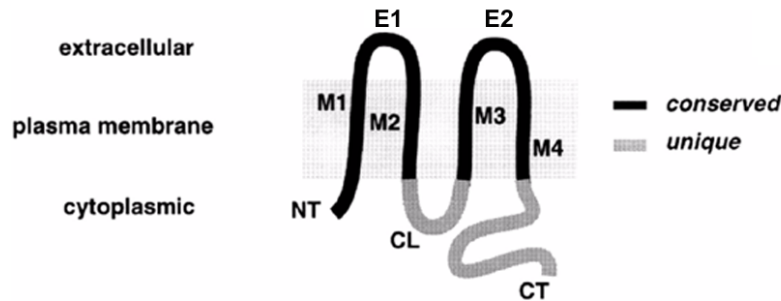
Fig.3 Schematic model of a connexin. Connexins are four times membrane crossing proteins with two extracellular loops and three cytoplasmic domains: N-terminus, intracellular loop and C-terminus. Taken from Nicholson et al., 1999.

Currently, 13 evolutionarily highly - conserved genes, which code for connexins, have been identified in mammalian tissues (White and Paul, 1999; Manthey et al., 1999; Teubner et al., 2001; Willecke et al., 2002). The same connexin can be expressed in different cell types and organs, and the same cell type can express different connexins.

Two connexons consisting of the same type of connexins can form a homotypic channel, whereas two connexons each consisting of different connexins can form a heterotypic gap junction channel. Connexin subunits within one connexon can form homo- or heteromeric hemichannels. Heterotypic or heteromeric connexin channels have permeability properties corresponding to those of the subunits, forming the channel (Martinez et al., 2002; Moreno, 2002; Beyer et al., 2001).

1.4 Intracellular trafficking of connexins

Connexins, as many other secretory proteins, are inserted co-translationally into the membrane of the endoplasmic reticulum (ER). On the way to the plasma membrane connexins pass through the Golgi network (Musil et al., 1991; VanSlyke et al., 2000; Martin et al., 2001). Brefeldin A, which disrupts the Golgi apparatus, prevents the trafficking of Cx32 and Cx43; however, Cx26 still reaches the cell surface (Martin et al., 2001). Hexamerisation of connexins is a prerequisite for their transport to the plasma membrane. Multisubunit assembly of connexins occurs after exit from the ER (Musil and Goodenough, 1993). The installation of connexons occurs predominantly into the nonjunctional plasma membrane. These PM connexons can move laterally and reach the margins of gap junction channels cluster (Lauf et al., 2002). Removal of gap junctions

from the plasma membrane occurs via endocytosis of the double membranous vesicle-like structures ("annular gap junctions") that are guided for degradation (Bjorkman 1962; Larsen and Tung, 1978; Ginzberg and Gilula, 1979; Laing and Beyer, 1995; VanSlyke et al., 2000).

1.5 Connexin phosphorylation

The majority of connexins are phosphoproteins (Traub et al., 1987,1989,1994; Crow et al., 1990, Musil at al., 1990; Saez et al., 1997, 1998). But only the phosphorylation of Cx43 is accompanied by an apparent molecular weight shift on SDS-polyacrylamide gels, forming a faster migrating, non-phosphorylated (NP) 43 kDa isoform and at least two slower migrating isoforms commonly termed P1 (45 kDa) and P2 (47kDa).
Cx43 is phosphorylated in the ER or cis-Golgi compartment, displaying the Cx43-P1 isoform. The existence of the P2 isoform correlates with the appearance of connexin43 on the plasma membrane and is necessary for the formation of functional gap junction channels (Musil and Goodenough, 1991;Laird et al, 1995).

Both, P1 and P2 isoforms contain predominantly phosphoserines (Crow et al, 1990).

Phosphorylation events can be involved in the oligomerisation of Cx43 into connexons, proper intracellular trafficking, formation and stabilisation of gap junctions, and degradation.

1.6 Connexin degradation

One of the most striking features of connexins is their rapid turnover. The half-life of Cx43 was found to be 1-3 h (Musil et al., 1991, 2000; Laird et al., 1991; Lampe, 1994). Such a dynamic turnover requires an efficient degradation mechanism to prevent the intracellular accumulation of Cx43.

As other transmembrane proteins, connexins are degraded in lysosomes after endocytosis. (Ginzberg and Gilula, 1979; Larsen et al., 1979). A study of Thomas and collegues (2003) suggests that the tyrosine-based motif of the C-terminus of connexin43 is responsible for lysosomal degradation of gap junctions.

A key question remained as to the role of proteasomes in the degradation of connexin. Recent studies revealed that proteasomal degradation would be the fate of the soluble pool of Cx43 dislocated from ER membranes (VanSlyke and Musil, 2002). It seems possible

that as a quality control step missfolded or mutant connexins can become ubiquitinated and degraded by proteasomes as they pass through the ER (Qin et al., 2003).

1.7 Interaction between connexins and protein partners

The intracellular transport of connexins, gap junction plaque assembly and stability, and modulation of channel activity are most likely governed by interactions with regulatory and structural proteins that recognize specific sequence motifs in the cytoplasmic domains of connexins. However, only few such connexin-interacting proteins have been described to date, which include the tight junction protein ZO-1, calmodulin, tubulin and certain protein kinases.

1.7.1 Calmodulin directly gates gap junction channels

Calmodulin (CaM) is a calcium-binding protein that is considered a major transducer of calcium signals. Many of the proteins that CaM binds are unable to bind calcium themselves, and use CaM as a calcium sensor and signal transducer. Increased calcium intercellular concentrations lead to binding of calcium by CaM, which subsequently undergoes a conformational change and binds to specific proteins for a specific response (James et al., 1995).

Recent data shows that CaM colocalizes with connexins and plays a direct role in gap junction channel gating (Peracchia et al., 1996, 2000; Sotkis et al., 2001; de Pina-Benabou et al., 2001).

Two cytoplasmically oriented sequences of Cx32, N-terminal (residues 1-21) and C-terminal (residues 216-230) have been shown to bind calmodulin in Ca^{2+}-dependent manner (Torok et al., 1997). In addition, the binding of CaM to Cx32 in the absence of calcium partially prevents its phosphorylation by the EGF receptor tyrosine kinase (Diez et al., 1998).

1.7.2 Association of connexins with Zonula occludens-1

Zonula occludens-1 (ZO-1) is a peripheral membrane protein of approximately 210-225 kDa, which is specifically enriched at tight junctions of epithelial and endothelial cells (Stevenson et al., 1986). ZO-1 tethers transmembrane proteins such as occludin, claudin and junctional adhesion molecules to the actin cytoskeleton (Denker and Nigam, 1998). It

is a member of the membrane-associated guanylate kinase (MAGUK) family of proteins, which consists of three distinct amino acid motifs, namely: **P**SD95/**D**lg/**Z**O-1 (PDZ) domains, an Src-homology-three domain (SH3) and a guanylate kinase domain (Gonzalez-Mariscal et al., 2000).

ZO-1 has been shown to associate with Cx43 in different cell types (Toyofuku et al., 1998, 2001; Giepmans and Moolenaar, 1998; Giepmans et al., 2001). Interaction with ZO-1 is dependent on the C-terminal isoleucine (DDLEI domain) of Cx43 (Giepmans and Moolenaar, 1998). Interesting, overexpression of a dominant-negative form of ZO-1, which is unable to associate with actin cytoskeleton, prevents Cx43 from localising to cell-cell contacts in cardiac myocytes, resulting in the decrease of electrical coupling via gap junctions (Toyofuku, 1998).

1.7.3 Cadherins facilitate the formation of gap junctions

Cadherins are transmembrane proteins whose extracellular domains promote calcium-dependent homotypic adhesion between neighbouring cells, whereas their cytoplasmic regions are linked to the actin cytoskeleton by means of cytoplasmic proteins called catenins: α-catenin, ß-catenin and γ-catenins (Aberle et al., 1996).

Cell adhesion molecules are obvious candidates to facilitate the formation of gap junctions. The large extracellular domains of cadherins would likely prevent their actual inclusion into gap junctional plaques, however cadherins can act to position opposing membranes for gap junction channel formation (Jongen et al., 1991). Recent data suggest the intriguing possibility that these two classes of cell surface proteins can interact via a signal transduction system. Cell lines, deficient for cadherins, show diminished communications via gap junctions, which can be corrected by transfection with DNA coding for the appropriate cell adhesion molecules (Musil et al., 1990). Depletion of N-cadherin, using si-RNA, lead to the redistribution of Cx43 from the cell surface to the cytoplasm (Wei et al., 2003). Cx43 can be co-immunoprecipitated with N-cadherin, and also with other N-cadherin-interacting proteins: α-actinin, α-catenin, p120 catenin, and LIN-7 (Wei et al., 2003; Singh and Lampe, 2003).

1.7.4 Protein kinases which phosphorylate connexin43

Connexin43 contains in their COOH-terminus a number of serin and tyrosin residues, which can be phosphorylated by several known and unknown protein kinases.

Oncogen v-Src tyrosin kinase promotes the direct phosphorylation of Cx43 on Tyr265 and Tyr247 in Cx43 (Kanemitsu et al., 1997, Lin et al., 2001). SH3 and SH2 domains of the v-Src mediate this interaction with Cx43, inducing the disruption of gap junctional communication (Loo et al., 1995; Swenson et al., 1990; Filson et al., 1990; Crow et al., 1990, 1992).

Proto-oncogen c-Src tyrosine kinase, which is activated via G protein-coupled receptors in mammalian cells, also closes gap junctions by phosphorylation of Tyr265 (Postma et al., 1998). Moreover, the interaction of c-Src SH2 domain with C-terminus of connexin43 in parallel abolishes the interaction of Cx43 with ZO-1 protein (Toyofuku et al., 2000).

PKCα can phosphorylate Cx43 on Ser368 and Ser372 in vitro (Saez et al., 1997). Ser368 is also a major site of phosphorylation in vivo. Phosphorylation of Cx43 on Ser368 decreases the number of cells transferring dye, enhances the relative frequency of a lower conductance state (~50 pS), and diminishes the relative frequency of the fully open state (~100pS) of gap junctions (Lampe et al., 2000).

A **cyclinB-dependent p34 cdc2 kinase** regulates phosphorylation of Cx43 in mitotic cells (Lampe et al., 1998; Kanemitsu et al., 1998). This unique phosphorylation results in the redistribution of Cx43 from the plasma membrane and the subsequent loss of gap junctions.

Agents, that upregulate cAMP level and activate **cAMP - dependent protein kinase (PKA)** result in increase of intercellular communications via gap junctions (Darrow et al., 1996; Ten Broek et al., 2001).

Activation of **mitogen-activated protein kinase (MAP)** induces phosphorylation of serine 279 and serine 282 of Cx43 and disruption of gap junctional communication (Warn-Cramer et al., 1996).

Casein kinase 1 (CK1) has recently been found to phosphorylate Cx43 in vitro (Cheng and Louis, 2001; Cooper and Lampe, 2002).

1.7.5 Connexins and cytoskeletal proteins

1.7.5.1 Tubulin

Microtubules play an important role in spatial organisation, cell polarity and directed movements of organelles in the cytoplasm. Connexons are delivered to the PM in vesicular carriers travelling along microtubules (Lauf et al., 2002). Cx43 forms complexes with β-tubulin in vitro (Giepmans et al., 2001). Nevertheless, nocodazole (drug widely used to disrupt microtubules) affects forward transport of Cx43 from the Golgi to the PM only minimally (Paulson et al., 2000; Martin et al., 2001) and does not influence dye coupling or propagation of calcium waves via gap junctions (Branes et al., 2002).

1.7.5.2 Actin

The morphological integrity of the actin cytoskeleton seems to be fundamental for the functional activity of gap junctions, probably because of associations among actin filaments, actin binding proteins and connexin43 at the plasma membrane.

Microinjection of anti-actin antibodies prevents translocation of Cx43 from the Golgi apparatus to the cell membrane and blocks dye coupling (Theiss and Meller, 2002). Disruption of microfilament by cytochalasin B inhibits the recruitment and assembly of Cx43 into gap junctions as indicated by fluorescence bleaching recovery experiments (Thomas et al., 2001). Several observations suggest that actin and myosin II are responsible for the removal of connexons from the plasma membrane (Murray et al., 1997). Other data propose a role of actin microfilaments for the process of clustering gap junctions into gap junctional plaques (Wang et Rose, 1995).

Cellular organisation is critical for the propagation of intercellular calcium signalling, mediated via gap junctions. Astrocytes in culture lost their capability for propagation of calcium waves when their actin cytoskeleton was disrupted by cytochalasin D treatment or affected by inhibition of myosin light chain kinase (Cotrina et al., 1998).

1.8 Connexin and signal transduction

Gap junctions are widely involved in the intercellular transfer of information. Second messengers like inositol 1,4,5-trisphosphate, calcium or cyclic nucleotides may diffuse through gap junctions thus modulating cellular physiological activities of neighbouring cells (Berridge, 1997; Boitano et al., 1992, 1998; Sanderson, 1995; Robb-Gaspers and Thomas, 1995; Leybaert et al., 1998; Niessen et al., 2000; Guthrie et al., 1999).

Recent studies indicate that connexin hemichannels are also active and that they might be essential in intercellular signalling beyond their incorporation into gap junctions. Astrocytes express functional hemichannels that mediate an extracellular release of ATP (Cotrina et al., 1998; Stout et al., 2002), NAD^+ (Bruzzone et al., 2001; Ebihara, 2003), glutamate and aspartate (Innocenti et al., 2000; Ye et al., 2003).

Connexin43 hemichannels, but not gap junctions, are the essential transducers of the extracellular signal-regulated kinase (ERK), activating anti-apoptotic effects of bisphosphonates. Bisphosphonates, drugs used widely in the treatment of osteoporosis, prevent osteocyte apoptosis by a mechanism involving ERK activation (Plotkin and Belido, 2001; Plotkin et al., 2002). This observation adds Cx43 to the list of transmembrane proteins capable of transducing survival signals in response to extracellular cues and raises the possibility that it may be involved in mediating effect of endogenously produced molecules or even drugs.

1.9 Dysfunction of connexins and human diseases

The importance of gap junctions for the multicellular organisms is highlighted by a wide array of different human diseases and mouse phenotypes that arise from defects of these genes. In humans, the inherited defects in individual connexin isoforms are associated with demyelinating disorders of the peripheral nervous system, severe hearing impairment, eye lens cataracts, skin disorders, heart arrhythmias, and heart malformation. Such of these diseases have a significant impact on the human population, with Cx26 mutations accounting for more than 50% of the cases of inherited asyndromic sensorineural deafness (Willecke at al., 2002).

Diseases result from the impaired interactions of connexins with their protein partners.

Disturbance of interaction with proteins of cellular trafficking machinery results in the absence of the wild-type connexins at the plasma membrane. In some cases connexins accumulate in the ER and induce a chronic endoplasmic reticulum stress response. Such a mechanism was suggested for the development of Charcot-Marie-Tooth peripheral neuropathy (Deschenes et al., 1997).

Disturbed protein-protein interactions of connexins with membrane-associated proteins also may lead to a major change in cell physiology and manifestation of diseases.

Thus, identification of new proteins, interacting with connexins provides a basis for clarifying the function of connexins at healthy and pathological conditions.

Mouse connexin	Major expression	Phenotype(s) of Cx-deficient mice	Human hereditary disease(s)	Human connexin
	n.a	n.a	n.a	hCx25
mCx26	breast, skin, cochlea, liver, placenta	lethal on ED11	sensorineural hearing loss, palmoplantar hyperkeratosis	hCx26
mCx29	myelinated cells	n.a	n.a	hCx30.2
mCx30	skin, brain, cochlea	hearing impairment	nonsyndromic hearing loss, hydrotic ectodermal dysplasia	hCx30
mCx30.2	n.a	n.a	n.a	hCx31.9
mCx30.3	skin	n.a.	erythrokeratodermia variabilis (EKV)	hCx30.3
mCx31	skin, placenta	transient placental dysmorphogenesis	Hearing impairment, erythrokeratodermia variabilis(EKV)	hCx31
mCx31.1	skin	n.a	n.a	hCx31.1
mCx32	liver, Schwann cells, olygodendrocytes	decreased glycogen degradation, increased liver carcinogenesis	CMTX, (hereditary peripheral neuropathy)	hCx32
mCx33	testis	n.a.		
mCx36	neurones	visual deficits	n.a.	hCx36
mCx37	endothelium	female sterility	n.a	hCx37
mCx39	n.a		n.a	hCx40.1
mCx40	heart, endothelium	atrial arrhythmias	n.a	hCx40
mCx43	many cell types	heart malformation	visceroatrial heterotaxia	hCx43
mCx45	heart, smooth muscle, neurones	lethal on ED10. 5	n.a	hCx45

mCx46	Lens	zonular nuclear cataract	congenital cataract	hCx46
mCx47	brain, spinal cord	n.a	n.a	hCx47
mCx50	lens	microphthalmia, zonular pulverulent and congenital cataract	zonular pulverulent cataract	hCx50
	n. a	n.a	n.a	hCx59
mCx57	ovaries	n.a	n.a	hCx62

Tab.1 Summary of currently known mouse and human connexin genes. Taken from K.Willecke et al., 2002.

Aim of this work

1. To identify new proteins, which are involved in the intercellular trafficking and plasma membrane appearance of connexin43.

2. To identify new proteins, interacting with connexin43, which are required for the functional activity of gap junctions.

3. To confirm these protein-protein interactions in live cells.

4. To analyse the functional importance of identified protein-protein interactions.

Materials

Chemicals

All chemicals used were of analytical grade and were purchased from Merck, Sigma, Boehringer or Serva.

Cell culture

Dulbecco's modified Eagle's medium (DMEM) was from Life Technologies, fetal calf serum from Biochrom/Seromed, trypsin-EDTA from Gibco BRL. Greiner provided all culture dishes. Oligofectamine for si-RNA transfection and Lipofectamine 2000 for cDNA transfection were from Invitrogen.

Antibodies

Polyclonal antibodies directed against connexin43 were from Sigma. Polyclonal antibodies against the first extracellular loop of connexin43 were raised in rabbits according to standard procedures. Polyclonal antibodies against the KDEL receptor were from Dr. I. Majoul (Dept. of Neurobiology, Max-Planck-Institute for Biophysical Chemistry, Göttingen, Germany). Monoclonal antibodies against drebrin (M2F6) were from StressGen and from Dr. T. Shirao (Gunma University Graduate School of Medicine, Maebashi, Japan).
Secondary antibodies coupled to Cy3 or Cy2 were purchased from Dianova.

Standard molecular biology components

Plasmid DNA extraction from *E. coli*, DNA extraction from agarose gel and purification of PCR products were performed with a Qiagen Spin MiniPrep or MaxiPrep Kit, a QIAquick Gel Extraction Kit, a PCR Purification Kit (Dianova). SuperSignal Substrate Kit (Pierce) was used for chemiluminescence.

Restriction enzymes were from Gibco /BRL, Boehringer or New England Biolabs. T4-polymerase and T4-DNA ligase from Amersham Pharmacia. Pfu polymerase was from Boehringer.

NAP10 and P20 columns (Amersham Pharmacia) were used for desalting/rebuffering of synthetic oligonucleotides and proteins, respectively. Nitrocellulose membranes for Western blotting were from Sartorius, polyvinylidene-difluoride (PVDF) membranes from Millipore. Glutation Sepharose 4B and Protein A Sepharose came from Amersham Pharmacia, protease inhibitors mix "Complete" was from Roche.

cDNA and fluorescent protein constructs

Connexin43 cDNA was from Dr. K. Willecke (University of Bonn, Germany), cDNA coding for drebrin-GFP from Dr. T. Shirao (Gunma University Graduate School of Medicine, Maebashi, Japan), GFP-actin from Dr. S. Kuznetzov (University of Rostok, Germany), Sec13-YFP, Sar1 dn and ARF1, ARF1 Q71L-GFP and p23-CFP from Dr. R. Duden (University of Cambridge, UK)

The si-RNA duplex against drebrin was synthesised by Dharmacon (www.Dharmacon com.).

Plasmid vector pGEX-4T3 was from Amersham Pharmacia.

Bacterial *E.coli* strains: DH5α was from Gibco-BRL, XL1-Blue from Stratagene.

Mammalian tissue culture cell lines Vero (African green monkey kidney) and COS (SV-40 transformed African green monkey kidney) were from ATCC.

IPTG was used for induction of protein synthesis at 0.5 mM final concentration for liquid culture from 1 M filtered stock.

LatrunculinB (disrupts actin microfilament organisation) was used from a 5mg/ml stock in EtOH at 50 nM final concentration.

Lucifer yellow CH and calcein (Molecular Probes, Eugene, OR) were used for microinjection.

Frequently used buffers:

PBS (phosphate buffered saline):

NaCl	137 mM
KCl	2.7 mM
Na_2HPO_4	8.1 mM
KH_2PO_4	1.4 mM, PH 7.4

Cytomix buffer:

KCl	120 mM
KH_2PO_4	10 mM
EGTA	2 mM
$MgCl_2$	5 mM
Hepes	25 mM
$CaCl_2$	0.15 mM
GSSG	5 mM
ATP	2 mM, PH 7.4

4. Methods

4.1 Construction of pGST-CT-Cx43

To create the GST-COOH-terminus-Cx43 (GST-CT-Cx43) construct the relevant part of rat heart connexin43 cDNA was amplified by PCR. The sequences of the primers were as follows: forward primer: 5'-CTAGGGATCCAAGGGCGTTAAGGATCGCGTG AAG; reverse primer: 5'-CTAGGCGGCCGCTAAAATCTCCAGGTCATCAGG.

The PCR product was restricted with BamHI and Not I and ligated into the BamHI/Not I sites of pGEX-4T-3. This placed the C–terminus of Cx43 sequence in frame with the upstream GST sequence. The correct sequence of the GST-CT-Cx43 construct was verified by DNA- sequencing.

```
1                        atgggtgac tggagtgcct tggggaagct tctggacaag
40  gtccaagcct actccaccgc tggagggaag gtgtggctgt cagtgctctt catattcaga
101 atcctgctcc tggggacagc tgttgagtca gcttgggggtg atgaacagtc tgcctttcgc
161 tgtaacactc aacaacctgg ctgcgaaaac gtctgctatg acaagtcctt ccccatctct
221 cacgtgcgct ctgggtcct tcagatcata ttcgtgtctg tgcccaccct cctgtacttg
281 gcccatgtgt tctatgtgat gaggaaggaa gagaagctaa acaagaaaga agaggagctc
341 aaagtggccc agactgacgg ggtcaacgtg gagatgcacc tgaagcagat tgaaatcaag
401 aagttcaagt acgggattga agagcacggc aaggtgaaaa tgaggggcgg cttgctgaga
461 acctacatca tcagcatcct cttcaagtct gtcttcgagg tggccttcct gctcatccag
521 tggtacatct atgggttcag cttgagcgcg gtctacacct gcaagagaga tccctgcccc
581 caccaggtag actgcttcct ctcacgtccc acggagaaaa ccatcttcat catcttcatg
641 ctggtggtgt ccttggtgtc tctcgctttg aacatcattg agctcttcta cgtcttctt**c**
**701 aaaggcgtta aggatcgcgt gaagggaaga agcgatcctt accacgccac cactggccca**
**761 ctgagcccat caaaagactg cggatctcca aaatacgcct acttcaatgg ctgctcctca**
**821 ccaacggctc cactctcgcc tatgtctcct cctgggtaca agctggttac tggtgacaga**
**881 aacaattcct cgtgccgcaa ttacaacaag caagctagcg agcaaaactg ggcgaactac**
**941 agcgcagagc aaaatcgcat ggggcaggcc ggaagcacca tctccaactc gcacgcccag**
**1001ccgttcgatt tccccgacga caaccagaat gccaaaaaag ttgctgctgg acatgaactc**
**1061cagccattag ccatcgtgga ccaacgacct tccagcagag ccagcagccg cgccagcagc**
**1121aggcctcggc ctgatgacct ggagat**tta
```

Fig. 4 Sequence of connexin43 gene (NCBI accession number x06656). C-terminus of Cx43 (aa$_{234}$-aa$_{382}$) used for cloning into pGEX-4T-3 shown in bold.
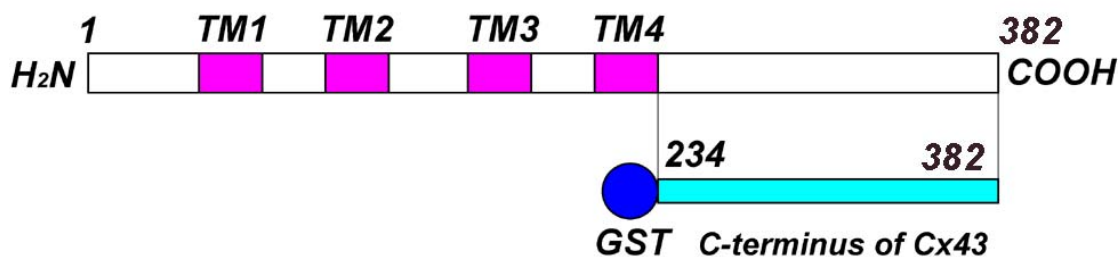
Fig.4 Schematic representation of connexinx43 and GST-C-terminusCx43 construct used in pull down experiment.

4.2 Expression and purification of GST-CT-Cx43 protein

LB medium (5ml) with 50 μg/ml ampicillin was inoculated with 1 colonie of *E.Coli* harbouring the vector construct pGEX-CT-Cx43 and incubated for 8h at 37°C with shaking about 200 rotation/min. 1 liter of LB medium with 50 μg/ml ampicillin was inoculated with 1ml of the preculture and incubated overnight at 24°C with shaking at about 200 rotations/min till an A_{600} of 1.0 −1.2. 0.5ml of 1M IPTG was added to induce synthesis of GST-fusion protein. After 3h cells were harvested by centrifugation at 5,000x g for 5min at 4°C, washed in ice-cold PBS and centrifuged again under the same conditions. Bacterial sediments were resuspended in 20 ml of ice-cold PBS containing 1 tablet of protease inhibitors mix "Complete" and 20 mg lysozyme and incubated on ice for 15min. Then cells were disrupted by sonication (15 bursts 5 times at maximum output setting) on a Branson model 250 Sonifier while the sample was kept in an ice-water mixture.

Triton X-100 (final concentration 1% (v/v)) was added and the lysate was incubated for 30 min on ice with gentle agitation. Thereafter, the sample was spun at 12,000x g for 10 min at 4°C. The supernatant was added to 1ml of a 50 % slurry of Glutathion Sepharose 4B in PBS. Then the sample was rotated for 30min at 4°C for binding GST-fusion protein to Glutathion Sepharose beads. After this procedure the sample was spun for 5 min at 500x g, the resin was collected and washed again 5 times with 20 ml each of cold PBS.

Where indicated the GST-fusion protein was eluted with elution buffer (5 mM Glutathion-SH in 50 mM Tris HCl, 50 ml, pH 8.0). 1 ml of elution buffer was added to the resin, the mixture was rotated for 5min at RT, spun at 500x g for 3 min, and the supernatant transferred to a fresh tube. The elution step was performed twice more, using the same resin. The eluted GST-CT-Cx43 protein fractions were combined, aliquoted, and stored at –80°C.

4.3 Preparation of fractions for pull down assay

The fresh mouse organs (brain, kidney, liver, spleen, and heart) were homogenised with 2 ml of " Cytomix" buffer containing the " Complete" protease inhibitor coctail. The homogenates were centrifuged in a Beckman TLA 100.3 rotor for 45 min at 50,000 rpm (about100,000 x g) at 4°C.

The supernatants were used in the experiments as "cytosolic fraction". The pellets were resuspended in 2 ml of the same buffer, but containing TritonX-100 to 1% and centrifuged under the same conditions. The supernatants were used in experiment as "membrane fractions".

4.4 Pull down using Glutathione Sepharose fusion protein

The cytosolic and membrane fractions were pre-cleared by incubating with 300 µl of Glutathione Sepharose 4B beads bound to GST for 1.5 h at 4°C on a rotating platform. The samples were centrifugated at 500x g for 3 min and the supernatant was used.

The pre-cleared cytosol was then incubated with 300µl of Glutathione Sepharose 4B beads bound to the GST-fusion protein for 1.5 h at 4°C on a rotating platform.
The beads were washed 5 times in " Cytomix " buffer containing " Complete " protease inhibitor coctail and 1% Triton X-100.
The samples were boiled for 2 min in 60 µl 2x SDS-PAGE sample buffer containing 0.1% (v/v) β-mercaptoethanol. The liquid phases were collected and 12% SDS-PAGE was carried out.

4.5 PCR

This method utilises a primer pair complementary to the respective 3´ ends of the region of interest in a double-stranded DNA template, a temperature stable DNA polymerase such as Taq polymerase and a thermocycler device to generate a vast amount of identical copies of the intervening sequence.

The annealing temperature (T) was determined for each primer pair separately by the following empirical relationship:

T (°C) = 69.3 + 0.41 x (GC%) - 650/l, where l = (overlap length in bases)

The lower of the two temperatures values for a primer pair was used in the reaction. Taq DNA polymerase activity was taken as 1000 bp per min.

Typical reaction mixture:

50 ng template DNA (~1µl)

50-100 pmol forward primer (1 µl)

50-100 pmol reverse primer (1 µl)

1 µl 10x dNTP mix

5 µl 10x Taq buffer

add double-distilled H_2O to 50 µl

mix

add 1 µl Taq polymerase

Typical PCR programme:

1. 94°C 4min   denaturation

2. 94°C 50 sec   denaturation

3. 62°C 25 sec   annealing

4. 72°C 30 sec   extension

5. 30 cycles steps 2 to 4

6. 4°C   cooling

4.6 DNA-gel electrophoresis

In TBE buffer (pH 8.1) the negatively charged DNA molecules migrate under the influence of an electrical field from the cathode to the anode. The distance migrated is dependent on fragment size and fairly independent of base sequence. The bands are made visible under ultraviolet light of 302 nm after staining of the gel with ethidium bromide solution.

TBE buffer:

50 mM Tris

1 mM EDTA

500 mM H_3BO_3

pH 8.1

Ethidium bromide 0.1 mg/ml

1% agarose gels were used. TBE buffer (100 ml) was added to 1 g of agarose and boiled in a microwave oven until the agarose had completely dissolved. After cooling to about 60° the gel was cast in a special chamber. To increase the density of the applied samples and to allow monitoring of the progress of the electrophoresis, 0.2 volume Blue marker was added to the samples. The gels were run in TBE at 70-80 mA for 10x10cm gels for about 60 min. Then gels were stained with ethidium bromide for 15 min. Documentation was performed with a Biometra CCD camera.

4.7 Purification of PCR products

DNA was purified using a QIAGEN extraction kit according to the manufacturer's instructions.

4.8 DNA sequence analysis

DNA sequence analysis was performed by the Sanger method by SecLab, Goettingen.

4.9 Estimation of DNA purity and concentration

DNA concentration was estimated from the absorption at 260 nm using a Gene Quant II (Pharmacia) device. For DNA concentration, the approximate relationship was used that an A_{260} of 1.0 corresponds to ca. 50 µg/ml double-stranded DNA, to 40 µg/ml single-stranded DNA, and to 31 µg/ml oligonucleotide DNA.

4.10 Restriction enzyme digestion

The DNA fragment coding a partial sequence of Cx43 (aa_{234}-aa_{381}) was digested with BamH1 and Not1.

Reaction mixture:

5 µg DNA

2 µl (20 unit) BamH1

2 µl (20 unit) Not1

6 µl restriction buffer

add H_2O to 60 µl

Incubation for 1h at $37^{o}C$

Restricted DNA was purified by gel electrophoresis followed by extraction from the gel.

4.11 Ligation

Sticky-end ligation was carried out at room temperature for 2-4 h, typically using a 1:1 - 5:1 insert:vector molar ratio and T4 DNA ligase.

Typical reaction mixture:

150-300 ng insert DNA

50-100 ng vector DNA

5xT4 ligase buffer 4 µl

add H_2O to 19 µl

add 1 µl (400 unit) T4 DNA ligase

4.12 Preparation of competent *E. coli* cells for heat shock transformation

LB-medium (250ml) was inoculated with cells of the desired strain. Overnight culture was harvested at an A_{600} of 0.5-0.9 by centrifugation (4,000x g, 10 min at 4°C). The cells were cooled on ice for 30 min and then washed twice with ice cold water and once with 25 ml sterile filtered TB followed by centrifugation at 7,000 x g for 5 min at 4°C. Cells were then resuspended once more in 5 ml TB. Aliquots (300 µl) were taken and stored at -80°C in the presence of 7% (v/v) DMSO unless used immediately.

Transformation buffer:
PIPES 10 mM
$MnCl_2$ 55 mM
$CaCl_2$ 15 mM
KCl 250 mM
in bidest. water, pH 6.7 is set before addition of $MnCl_2$

4.13 Preparation of electro-competent *E.coli* cells

An overnight culture (1 ml) of *E.coli* XL1-Blue cells was used to inoculate 1 l of fresh LB medium. The culture was grown at 37°C with agitation for about 2.5 h untill an A_{600} of 0.5-0.8 was achieved. The flask was cooled on ice for about 30 min, and the cells were collected by centrifugation at 4,000 x g for 20 min at 4°C. The cells were washed subsequently with 1 l of ice cold sterile HEPES buffer, 500 ml HEPES buffer, and 20 ml HEPES buffer with 10% (v/v) glycerol, followed by centrifugation. Finally cells were resuspended in 2-3 ml sterile 10% (v/v) glycerol and aliquoted. Samples (100 µl) were frozen on dry ice and stored at −80°C.

HEPES buffer: 1 mM HEPES, pH 7.0
HEPES/glycerol: 1 mM HEPES, pH 7.0; 10% (v/v) glycerol
10 % glycerol: 10 % (v/v) glycerol in bidest. water
All solutions were sterilised by autoclaving before use.

4.14 Transformation of *E.coli* by electroporation

Electro-competent *E.coli* XL1-Blue cells (50 μl) were thawed on ice and transferred to a chilled 0.1 cm electroporation cuvette. Plasmid DNA (1.0 μg) was added. The cuvette was placed into a Gene Pulser electroporator (BioRad) and pulsed once with 1800 V, 25 μF, 20 Ohms. The discharge time was usually about 4,5 - 5 ms. 1 ml LB medium was added immediately after electroporation and the sample was incubated with agitation at 37°C for 1h. 100 μl of this culture were plated onto LB-Ampicillin or LB-Kanamycin plates and incubated overnight at 37°C.

4.15 Precepitation of DNA using plasmid mini and maxi-preps

Small- or large-scale plasmid extractions were performed using Plasmid Mini-and Maxi-Prep kits from Quiagen according to the manufacturer's recommendations. The basic principle involves alkaline lysis of the cell wall, degradation of RNA by RNase, precipitation of proteins and chromosomal DNA with high salt, binding of plasmid DNA to a silica-gel matrix, elution and precipitation with isopropanol and ethanol.

4.16 Antibodies
4.16.1 Covalent linking of peptides to carrier protein using the bifunctional reagent sulfo-SMCC

Keyhole limpet hemocyanin (KLH, Pierce) was used as a carrier protein for synthetic peptides. Synthetic peptide raised against the first extracellular loop of connexin43 (aa46-aa68) was coupled via their C-terminal Cys residues to primary amines (mainly to Lys side chains) using the bifunctional reagent sulfosuccinimidyl 4-(N-maleimidomethyl) cyclohexane-1-carboxylate (sulfo-SMCC, Pierce).
20 mg of KLH in 2 ml bidest. H_2O was activated by incubation with 3 mg sulfo-SMCC (dissolved in 200 μl dH_2O) for 45 min at RT under argon. The sample was then run over a G-25 column to remove non-reacted sulfo-SMCC and the first peak, measured at 280 nm, was pooled. The pH of the pooled fractions was then set to 7.15. The coupling reaction was initiated by adding 20 mg of the Cys-containing peptide, dissolved in bidest. H_2O, and the mixture allowed to proceed for ca. 5 h at RT with end-over-end rotation.

Thereafter, the sample was dialysed extensively against PBS, aliquoted into 500 μg protein aliquots, and stored at -20°C until used for immunisation.

4.16.2 Rabbit immunization

Initially 10 ml of blood was taken before the first immunisation to obtain pre-immune serum. For the first injection, 500 μg of coupled peptide, 1 ml Freund's complete adjuvant and 50 μg muramyl dipeptide were mixed to get a thick emulsion. This suspension was injected subcutaneously and intracutaneously according to standard procedure.

4.16.3 Purification of antibodies

Anti-serum (10 ml) was applied to a column holding 1 ml of Protein A Sepharose pre-washed with PBS. Binding of IgG proteins was allowed to proceed overnight at 4°C by slowly circulating the serum repeatedly over the column with the aid of a peristaltic pump. The column was then washed with PBS until all unbound proteins had been washed out (measured at A_{280}). Bound IgG was eluted in one step with 3 ml 100 mM sodium citrate (pH 3.2). Eluted proteins were collected in 1.5 ml tubes already containing sufficient neutralisation buffer (300μl 1 M Tris/HCl, pH9.0) for immediate neutralisation.

4.17 Determination of protein concentration

Protein concentrations were estimated according to Bradford (Bradford, 1976). Briefly, the absorption of a protein-specific dye, Coomassie Brilliant Blue, is measured near 595 nm. This absorption, which is due to interactions with basic or aromatic residues, yields relatively good linear concentration dependence for most soluble proteins. Protein solutions of unknown concentration are measured and the absorbance plotted against a reference curve obtained with a protein of known concentration (BSA). From this an approximate concentration is determined.

Staining solution:
100mg Coomassie Brilliant Blue G 250
50 ml 95% (v/v) ethanol

100 ml 85% (v/v) phosphoric acid

add H_2O to 1 litre and filter the solution.

The dye was first dissolved in ethanol before addition of the other components. The solution was filtered before use. A few (1-10) µl of the protein sample were added to1 ml dye solution. The mixture was incubated for 5 min at room temperature and OD at A_{578} was measured. As reference, an identical amount of protein solvent solution was treated similarly. Determination of the protein concentration was based on the concentration curve of bovine serum albumin (1-10µg) from which the factor of the staining solution was calculated. The factor is the ratio of the weight of bovine serum albumin to OD at A_{578} in the linear region of the standard curve.

Protein concentration (µg/µl)= (ΔOD x Factor x Dilution) / Volume of protein solution

4.18 Subcellular fractionation of cultured cells

Vero cells (ATCC) grown in a monolayer for 36 h in a 14.5 cm Peri dish were surface-biotinylated on ice for 10 min. Excess of unbound biotin was removed by washing the cells with ice-cold PBS. Cells were detached from Petri dishes after exposure to 10 mM EGTA in PBS and transferred on ice into "internal medium".

"internal medium":

K glutamate	130 mM
sucrose	20 mM
NaCl	20 mM
EGTA	2 mM
ATP	2 mM
glutathione	5 mM

pH 7.6

To preserve the integrity of subcellular organelles, cells were disrupted gently by sequential pushing them through injection needles of decreasing diameter: 22-, 24- and 27-G x. Cell homogenate was centrifugated for 10 min 3,000 x g at 4^0C and postnuclear

supernatant (PNS) was collected. Then PNS was separated on a Nycodenz step gradient: 1 ml of each : 40, 30, 25, 15, 12.5, 10, 7,5, 5, and 2.5% (v/v) Nycodenz in internal medium. After centrifugation at 120,000 x g_{av} for 1 h at 4 °C in a SW 40.1 rotor 9 fractions (+1 bottom fraction) were collected from the top and analysed for total protein concentration. The gradient fractions were diluted with internal medium and spun again for 2h at 100,000x g_{av} to separate membranes and soluble proteins in each fraction. The pellets obtained from each fraction were dissolved in "internal medium" in the presence of 1% Triton X-100 and were used for immunoblotting and immunoprecipitation.

Biotinylated fractions (indicating an enrichment of plasma membrane) were detected after transfer to PVDF membranes with streptavidin-peroxidase. Golgi fractions were detected by immunoblotting with anti-ERD2 antibodies. ER fractions were detected by immunoblotting with anti-KDEL antibodies.

4.19 Immunoprecipitation

Plasma membrane and Golgi membrane fractions were obtained from the gradient centrifugation. Fractions were dissolved in the internal medium in the presens of 1% Triton X-100, then fractions were precleared by incubation with 50 µl protein A Sepharose for 1h at 4°C under rotation. Precleared fractions were incubated with 5 µl anti-Cx43 antibodies, developed against the first extracellular loop (aa_{46}-aa_{68}) for 2h at 4°C on a rotating platform, and then with 100 µl Protein-A-Sepharose under the same conditions.

After washing, samples were boiled for 2 min in 50 µl 2x SDS-PAGE sample buffer. The liquid phases were collected and 12% SDS-PAGE was carried out.

4.20 Denaturating polyacrylamide gel electrophoresis (SDS-PAGE)

The detergent sodium dodecyl sulphate binds to proteins at an average of one SDS molecule per two amino acid residues. SDS denaturates the proteins, dissociates protein complexes and imparts the negative charge of polypeptide chains. Reducing agents such as dithiothreitol (DTT) or 2-mercaptoethanol are used to reduce cystines (disulphide bonds). The electrophoretic mobility of SDS-protein complexes is inversely proportional to the logarithm of the molecular mass of the protein.

Solutions:

Stacking gel buffer:

Tris/HCl 0.5 M

In H_2O bidest., pH 6.8

Resolving gel buffer:

Tris/HCl 1,5 M

SDS 0.4 % (w/v)

In H_2O bidest., pH 8,6

APS : Ammoniumpersulphate 40% (w/v) in H_2O bidest

SDS: 10% (w/v) in H_2O bidest

TEMED: 60% (w/v)

Running buffer:

Tris base 25mM

Glycin   190mM

SDS   0.1%(w/v)

	12% resolving gel	5% Stacking gel
H_2O	5 ml	4.7 ml
Resolving gel buffer	3.75 ml	-
Stacking gel buffer	-	3.4 ml
Acrylamide+bisacrylamide 30%	6 ml	1.4 ml
SDS10%	150 µl	100 µl
APS40%	37.5 µl	37.5 µl
TEMED	15 µl	10 µl

Tab.2 Preparation of 12% resolving and 5% stacking gels for SDS-PAGE.

Solutions for resolving gel were mixed according to the Tab.2 and poured immediately after addition of TEMED and APS, up to 2 cm from the top of the gel cassette. A few drops of isopropanol were added to prevent desiccation of the gel. After polymerisation isopropanol was rinsed off and a freshly prepared stacking gel solution added. Slots where formed by placing of the comb. Gel cassette was transferred to the electrophoresis chamber (BioRad) with running buffer; markers and protein samples were inserted into the hollows. A constant 25 mA current was applied untill the bands reached the bottom of the gel.

4.21 Staining of proteins at the SDS-PAGE

Gels were stained in Coomassie blue staining solution for 2 hour at room temperature followed by reduction of the background using destaining solution 1 for several hours at room temperature. Gels were rehydrated by equilibration in destaining solution 2.

Staining solution:

Coomassie brilliant blue R250 2 g

Coomassie brilliant blue G1 0.5 g

Ethanol 425 ml

Methanol 50 ml

Acetic acid 100 ml

H_2O bidest. 425 ml

Destaining solution 1:

Ethanol 450 ml

Acetic acid 100 ml

H_2O bidest 450 ml

Destaining solution2:

Acetic acid 70ml

H_2O bidest. 930ml

4.22 Immunoblotting

4.22.1 Western blotting onto nitrocellulose membranes

After completion of electrophoresis the polyacrylamide gel was removed and placed on top of two sheets of Whatman filter paper and a nitro-cellulose membrane (0.2 μm pore diameter) pre-equilibrated in blot buffer. After carefully removing of air bubbles, other two sheets of Whatman filter paper pre-equilibrated with blot buffer, were applied on top. The transfer sandwich was set up on the cathode plate of the chamber in the corresponding position and covered with a lid comprising the anode. For an 8x6x0.1 cm gel, transfer was carried out at 100 mA constant current for 1 hour.

Blot buffer:

25 mM Tris/HCl, pH 8.3

192 mM glycine

20 % (w/v) methanol

4.22.2 Western blotting onto PVDF membranes

Immobilon-P PVDF (polyvinylidene difluoride) membranes (Millipore) were used. The transfer sandwich was composed of:

1. Whatman filter paper equilibrated for a few minutes in anode buffer 1;

2. Whatman filter paper equilibrated for a few minutes in anode buffer2;

3. PVDF membrane activated for a few seconds in methanol, washed for

2-3 min in double-distilled water and equilibrated for 5 min in anode buffer 2;

4. Separating gel equilibrated for 5 minutes in cathode buffer;

5. Whatman filter paper equilibrated for a few minutes in cathode buffer.

Transfer was carried out as for nitrocellulose blots.

Anode buffer 1:

0.3M Tris/HCl, pH 10.4 at RT

20 % (v/v) methanol

Anode buffer2:

25 mM Tris/HCl, pH 10.4 at RT

20 % (v/v) methanol

Cathode buffer:

25 mM Tris/HCl, pH 9.4

20 % (v/v) methanol

4.22.3 Immuno-staining of Western blots

Blocking solution:

0.1 % Tween

1 % low fat milk in PBS

Washing solution:

0.1 % Tween in PBS

The blotted membranes were washed with blocking solution for 1h at RT to saturate unspecific protein binding sites on the membrane and then incubated with primary antibodies (generally at 1:5000 dilution) in 10 ml of the fresh blocking buffer for 1h at RT. After 3 times washes (20 min each) with washing solution the membranes were incubated with horseradish peroxidase coupled secondary antibodies (goat anti-rabbit or goat anti-mouse, diluted 1: 2000 in 10 ml of the fresh blocking buffer) for 1h at RT. Then membranes were washed again 3 times (20 min each) with washing solution and 3 times with PBS.

4.22.4 Chemiluminescence

Detection by chemiluminescence was performed using the Super Signal Substrate kit (Pierce) as recommended by the manufacturer. The method utilises a peroxide solution as substrate for horseradish peroxidase and a Luminol/enchancer solution for amplification of the signal. The signal was recorded by Fujifilm LAS-1000 cooled CCD camera and analysed using Aida image analysis software (Fuji).

4.23 Protein sequencing

Protein bands, obtained from pool down assay were excised from the gels. Each band was digested with trypsin and sequenced utilising MALDI Q-TOF mass spectrometry by Dr. Kathryn Lilley (Proteomics Center, Cambridge).

4.24 Mammalian cell culture techniques

4.24.1 Cell culture

Vero cells, COS cells and mouse astrocytes were cultivated in DMEM supplemented with 10 % FCS, 100 U/ml penicillin, 0.1 mg/ml streptomycin, 100 mM L-glutamine, 100 mM sodium pyruvate. Cells were grown at 37°C under 5 % CO_2 and 95 % humidity. Vero cells were stored at -170^0C under liquid nitrogen in 10% DMSO in DMEM containing 20% FCS. Vero cells were used not more than 20 first passages. Mouse astrocytes were used as primary culture not more than 4 passages.

4.24.2 cDNA transfection of cultured cells by electroporation

Transfection buffer ("cytomix"):

KCl 120 mM

KH_2PO_4 10 mM

EGTA 2 mM

$MgCl_2$ 5 mM

Hepes 25 mM

$CaCl_2$ 0.15 mM

GSSG 5 mM

ATP 2 mM

Cells were grown in14 cm Petri dishes to 80 % confluence, washed twice with PBS, detached by trypsin treatment, resuspended in 10 ml PBS and centrifuged at 1,000 rpm for 3 min. Cell pellets were resuspended in 1 ml transfection buffer. 350 μl of cell suspension was transferred to 0.2 cm electroporation cuvette together with 15 μg of

cDNA. The cuvette was placed into a Gene Pulse electroporator (BioRad) and pulsed once with 0.7 kV, 50 μF, and 200 Ohms. The time constant was usually about 1.4 ms. 15-20 min after transfection cells were resuspended in the medium and plated again. The expression of plasmid-coded proteins was examined 6-24 h after tranfection.

4.24.3 cDNA transfection using Lipofectamine 2000

Astrocytes where transfected in the presence of Lipofectamine 2000. For transfection 50 μl of Optimem containing 1μg of DNA were mixed with 50 μl of Optimem containing 2 μl of Lipofectamine 2000 and added 20 min after mixing to cells growing on one cover slip (diameter12 mm). Then cells were incubated at 37°C under 5 % CO_2 and 95 % humidity. After 4-5 hours DMEM medium was exchanged for DMEM without Lipofectamine 2000. Protein expression was examined 12-24 h after transfection.

4.24.4 si-RNA transfection

RNA interference (si-RNA) is a highly conserved gene silencing mechanism that uses double-stranded RNA (dsRNA) as a signal to trigger the degradation of homologous mRNA. si-RNA oligos directed against Drebrin mRNA (5´CCAGAAGGUGAUGUACGGCdTdT 3´ sense and 3´dTdTGGUCUU CCACUACAUGCCG 5´antisense) nonlabeled or labelled with Cy3 at the 5'sense end were produced by Dharmacon (www.Dharmacon com.).

Oligofectamine reagent (Invitrogen) was used for si-RNA transfection according to the manufacturer's instruction. For one well d = 24-30mm 20 μl of Oligofectamine and 20 μl of 20 μM si-RNA was taken. For co-transfection of si-RNA and DNA, cells were electroporated as described earlier except that the buffer was prepared with deionised RNase-free water. Expression patterns were analysed by immunofluorescence, western blotting, dye transfer and electrophysiology 10, 24,and 48 hours after transfection.

4.25 Indirect immunofluorescence

Blocking solution: 0.1 % saponin in PBS
Permeabilizing solution: 0.1 % saponin/3% BSA in PBS.

Cover slips with cells grown to about 80% confluency, were transferred to 24 well plates, washed 3 times with PBS, and fixed with 4 % paraformaldehyde in PBS for 15 min at RT. The fixed cells were treated for 10 min with 50 mM NH$_4$Cl to inactivate free aldehyde groups, and washed twice with PBS. Cells were then incubated in blocking solution for 10 min at 37°C and subsequently in permeabilising solution for 10 min at 37°C. Incubation with primary antibodies was carried out in a humidity chamber at 37°C for 1h at a dilution of 1:100. Thereafter cells were sequentially washed with permeabilizing solution, blocking solution, and PBS. Incubation with Cy3- (or Cy2-) labeled secondary antibodies was performed under the same conditions. After washing cells were mounted with Dako fluorescence mounting medium and analysed by fluorescence microscopy.

4.26 Fluorescence- and immunofluorescence microscopy and image processing

Fluorescence microscopy was performed with Zeiss LSM410 fluorescence microscope equipped with 100x 1.4 NA oil immersion Plan Achromate objective, a CCD-camera (Kodak, Princeton Instruments Inc.)

Filter set was:

GFP and Cy2: excitation BP 470/20, emission BP 505/530;

Cy3: excitation BP 546/2, emission BP 575-640;

CFP: excitation BP 430/20, emission BP 485/17;

YFP: excitation BP 500/20, emission BP 535/30.

Acquired images were documented and analyzed using MetaMorph 6.0 (Universal Imaging Corporation, West Chester, PA) and Adobe Photoshop 5.0.

4.27 FRET analysis

CFP-Drebrin (donor) and Cx43-YFP (acceptor) were co-expressed in Vero cells for 12 h. FRET was estimated from the increase of donor fluorescence after acceptor bleaching. Images of Dbb (donor fluorescence before bleach) and Abb (acceptor fluorescence before bleach) were acquired with a Zeiss Axiovert 100 TV fluorescence microscope equipped

with 100x 1.4 NA oil immersion Plan Achromate objective, a CCD-camera (Kodak, Princeton Instruments Inc.), and CFP and YFP filter sets (Omega Optics and AF Analytic, Germany). An increase in donor fluorescence was monitored with the excitation filter set contained for excitation: BP 430/20, for emission: BP 485/17. The acceptor was photoinactivated using an Ar-Kr-ion laser (INNOVA 70C Spectrum, Coherent) laser $\lambda = 530$ nm. After bleaching two images: Dab (donor fluorescence after bleaching) and Aab (acceptor fluorescence after bleaching) were recorded. The wavelength $\lambda = 530$ nm ensured that CFP (max.excitation: $\lambda = 440$nm) was bleached only negligibly while more than 95% of the YFP (max.excitation: $\lambda = 515$nm) was bleached within 3 min. Images were analysed with the MetaMorph 6.0 program (Universal Imaging Corporation, West Chester, PA). Intensity of fluorescence of a CFP-drebrin (donor) and Cx43-YFP (acceptor) before and after bleaching was shown using the linescan and 3D-profilescan trough the region of cell-cell contact. As a negative control the unchanged background region was depicted before and after the acceptor bleaching.

4.28 Electron microscopy of ultrathin cryo-sections

Electron microscopy of ultrathin cryo-sections was kindly performed by Dr. Dirk Wenzel, Max-Plank- Institute of Biophysical Chemistry, Goettingen, Germany. Shortly, Vero cells were co-transfected with Cx43-YFP and CFP-drebrin or si-RNA against Drebrin. For immunolabeling, ultrathin cryo-sections were incubated with anti-Cx43 or anti-drebrin antibodies for 1 h followed by a 30 min incubation with 10 or 5 nm colloidal gold-labeled goat-anti-rabbit or goat anti-mouse Fabs (British BioCell). Immunolabeled sections were examined with a Phillips CM120 electron microscope.

4.29 Microinjection

Calcein (1% in "Cytomix" solution) was microinjected using an Eppendorf microinjection system. Dye transfer was examined, using an inverse fluorescence microscope (IM35, Zeiss, Oberkochen, Germany) with filter set for excitation $\lambda = 494$ nm, for emission $\lambda = 517$ nm.

4.30 Electrical coupling analysis using double patch clamp in whole cell configuration

Coverslips with adherent cells were transferred from the culture dishes to the experimental chamber under an upright microscope (Axioskop, Zeiss) with phase-contrast optics, fitted with 2.5x plan/0.075 numerical aperture and 40x-W/0.80 objectives. The chamber was superfused with Krebs-Ringer solution.

Krebs-Ringer solution:

NaCl 140 mM

KCl 4 mM

$CaCl_2$ 2 mM

$MgCl_2$ 1 mM

glucose 5 mM

pyruvate 2 mM

HEPES 5 mM, pH 7.4 at RT

Patch pipettes were fabricated from borosilicate glass filaments (BioMedical Instruments) by means of a horizontal puller (DMZ-Universal, Zeiss-Instrument, München, Germany). When filled with electrode solution, the pipettes had a DC resistance of 2-5 MOhm.

Pipette solution:

KCl 140 mM

sodium aspartate 10 mM

MgATP 3 mM

$MgCl_2$ 1 mM

$CaCl_2$ 1,4 mM

EGTA 5 mM (pCa ~7.5)

HEPES 5 mM

In H_2O bidest., pH 7.2, filtered through 0.22-μm filters.

Experiments were carried out on pairs of cells using the dual voltage-clamp method in the whole-cell configuration. Electrodes were connected to separate clamp amplifiers EPC7 (ESF, Friedland) and EPC9 (HEKA Electronics, Lambrecht, Germany). Initially, the membrane potential of both cells was clamped to -70 mV. Voltage steps of 10 mV (from -160mV to $+170$ mV) were applied to cell 1 while cell 2 was kept at -70 mV. Current responses from both cells were recorded. Recordings were filtered at 3 kHz and digitized at 10 kHz, using the program PULSE, version 8.53 (HEKA Electronics, Lambrecht, Germany, EPC9) or Axograph 4.6 (Axon Instruments, USA, EPC7) and stored on the hard disks of two Macintosh computers for off-line analysis (Igor Pro). The coupling ratio between contacting cells was calculated as relation of current in cell 2 to current in cell 1 (I_2/I_1).

5. Results

5.1 Intracellular transport of connexin43

Connexins are relatively short living molecules (half-live 1-3h; Musil et al., 1990), which are co-translationally inserted into the endoplasmic reticulum (ER) membrane. Six connexin molecules oligomerise to form a connexon in the ER membrane. Connexons are transported through the Golgi network to the plasma membrane, where docking to connexons from neighbouring cells forms gap junctions. To investigate the transport of connexin43 from the ER to the plasma membrane, the Cx43 fused to green (Cx43-GFP), yellow (Cx43-YFP) or cyan (Cx43-CFP) fluorescent protein was expressed in Vero cells (Fig.5). ER-Golgi localisation of Cx43 fused to fluorescent protein was usually detected 4-5 h after transfection by electroporation (Fig.5 a), formation of gap junctional plaques was observed 6-10 h after transfection (Fig.5 b).
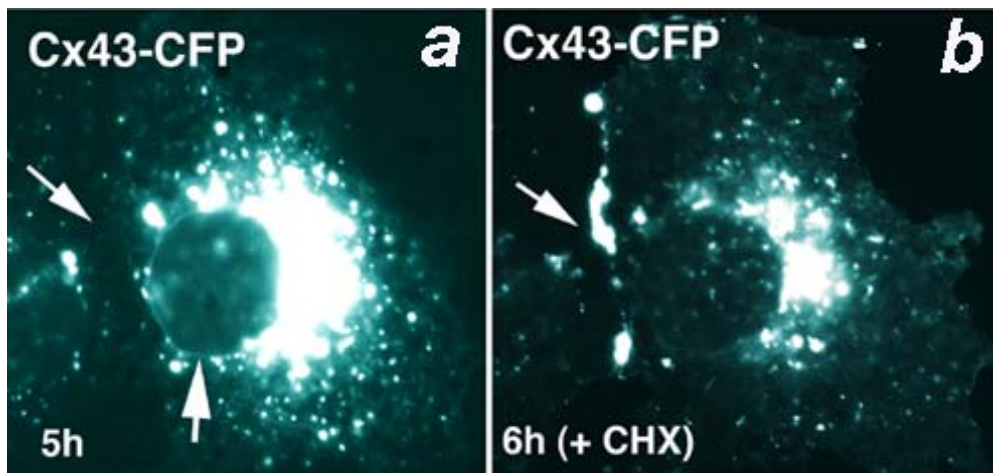

Fig.5 Intracellular transport of connexin43-CFP
a): Localisation of Cx43-CFP in the endoplasmic reticulum (ER) and Golgi region 5 h after transfection (arrows indicate presence of Cx43-GFP in the ER and absence at the contacting plasma membrane) .
b): Localisation of Cx43-CFP in the Golgi and formation of gap junctions between contacting cells (arrow) 6 h after transfection. Cycloheximide (CHX) was added to block new protein synthesis 5 h after transfection.

5.2 Involvement of small GTPases in the transport of connexin43

Small GTPases are involved in the formation of transport vesicles on the surface of either the ER, the Golgi complex, or endosomes. The small GTPase Sar1 is responsible for the initiation of COPII-dependent transport of vesicles from the ER membrane (Aridor et al.,

2001). The small GTPase ARF-1 (ADP-ribosylation factor) regulates the formation of COPI coated secretory vesicles from the Golgi network (Pepperkok et al., 1998; Spang et al., 2002). Involvement of small GTPases in the transport of connexin43 was analysed. Experimental data revealed that overexpression of the GTP-restricted mutant of Sar1p in Vero cells blocked transport of connexin43 from the ER to the Golgi (Fig.6). Moreover, Cx43 accumulated in the ER release sites, colocalising with Sec13 (Fig.7). Sec 13 is a protein of the COPII complex, which initiates membrane deformation and vesicle budding, and a marker of ER-release sites (Hobman et al., 1998; Tang et al., 2001).

The GTP-bound form of ARF1 (ARF1Q71L) blocked exit of Cx43 from the Golgi, preventing its appearance on the plasma membrane (Fig.8).
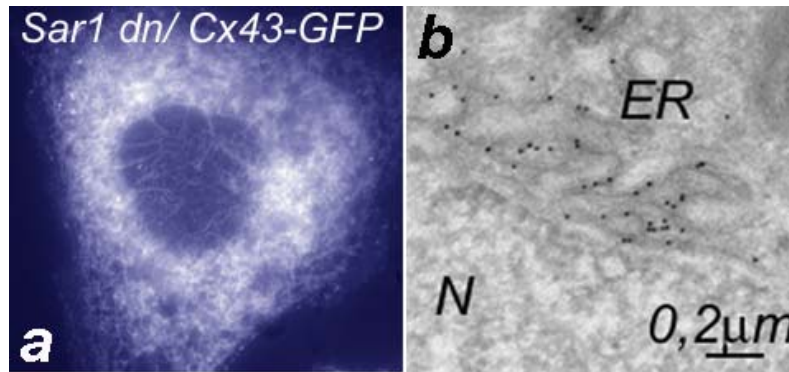

Fig.6 a): Expression of Sar1 dn prevents exit of Cx43-GFP from the endoplasmic reticulum. In Vero cells coexpressing Sar 1 dn and Cx43-GFP (10 h after transfection) Cx43-GFP was present only in the ER. In control Vero cells, transfected with Cx43-GFP plasmid only, Cx43-GFP was present in the Golgi and at the plasma membrane, like in Fig.5, b.
b): Immuno-electron microscopy image of a Vero cell, coexpressing Sar 1 dn and Cx43-GFP. Accumulation of Cx43-GFP in ER membranes was detected with anti-Cx43 antibodies.
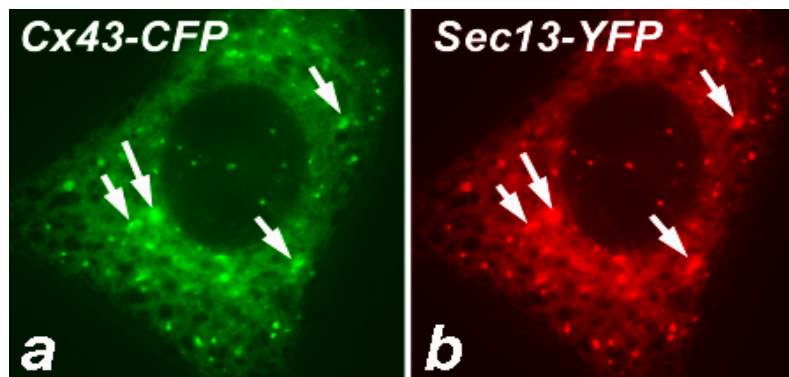

Fig.7 Cx43-CFP accumulates in ER- release sites in Sar1 dn expressing Vero cells (12 h after transfection) as indicated by colocalisation with Sec13 (arrows).
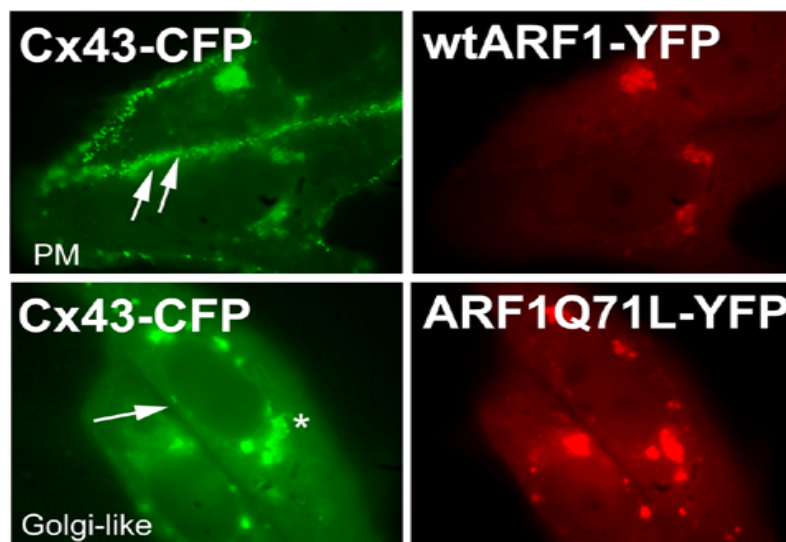
Fig.8 Vero cells, co-expressing Cx43-CFP and wild type or mutant ARF1-YFP (12 h after transfection). Overexpression of wild type ARF1 does not affect the transport of Cx43-CFP from the Golgi to the PM (upper panel). Overexpression of ARF1 Q71L blocks exit of Cx43-CFP from the Golgi and prevents appearance of gap junctions on the plasma membrane (lower panel).

5.3 Pull down assay with GST-CT-Cx43, protein sequencing and identification of drebrin as a Cx43-interacting protein

In search for new interaction partners of Cx43 we used a proteomics approach to screen subcellular fractions from different mouse tissues (brain, kidney, lung, heart, liver) for proteins that may interact with a GST-fusion protein encompassing the COOH-terminal domain of Cx43 (residues 234-382), which is normally exposed to the cytosol. Pull-down assays using this Cx43-COOH terminal domain GST-fusion protein recovered several bands that were resolved by SDS-PAGE and visualised with Coomassie Blue (Fig.9). MALDI/ Q-TOF (matrix assisted laser desorption ionisation/ quadripole time of flight) mass spectrometry analysis of tryptic peptides identified a number of candidate interacting proteins. One of them, drebrin E, was reproducibly recovered in pull-down assays from brains membrane fractions using the Cx43-GST fusion protein. Together, 22 peptides with exact matches to the cDNA-derived protein sequence of drebrin were obtained by Q-TOF sequence analysis (Tab.3).
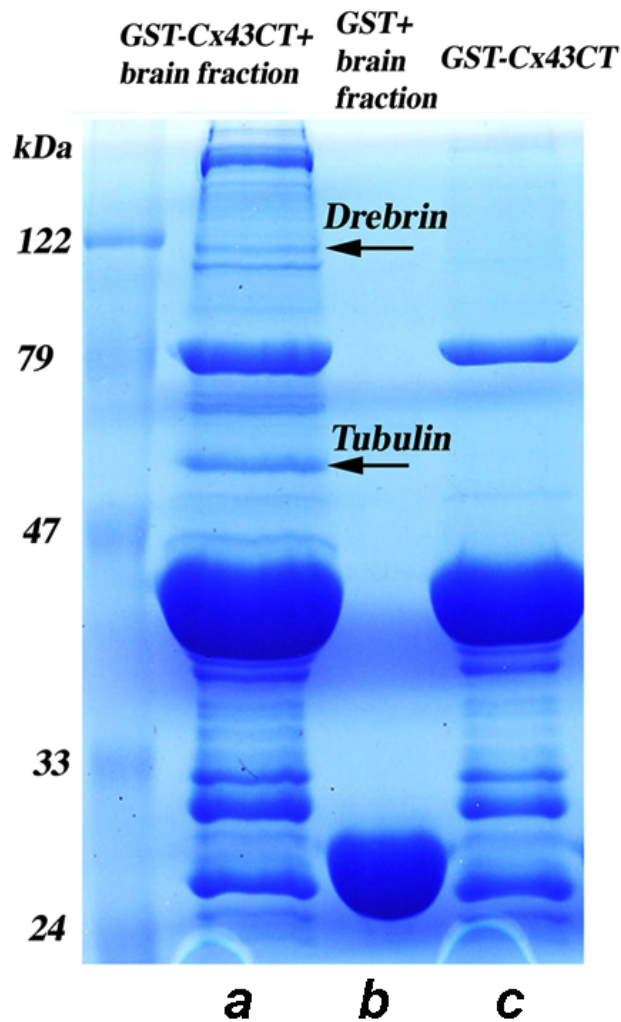
Fig.9 Result of pull down experiment using the GST-Cx43-C-terminal construct (aa $_{234}$- aa$_{382}$) and a membrane fraction of mouse brain homogenate.
 SDS-PAGE: a) pull down with GST-Cx43-C-terminal construct and a membrane fraction of mouse brain homogenate; b) control pull down with GST alone and a membrane fraction of mouse brain homogenate; c) GST-Cx43-C-terminal construct. Arrows indicate position of drebrin and β-tubulin in the pulled down fraction.

Nr.	matched peptide	amino acid number in drebrin sequence	score
1	DSQAALPK	72-78	18
2	MAPTPIPTR	330-338	55
3	EQFWEQAK	178-185	40
4	EQSIFGDQR	53-61	76
5	VMYGFCSVK	63-71	14
6	DEEEESQMK	262-270	13
7	QQSLEAEEAK	239-248	101
8	LELLAAYEEV	11-20	100
9	YVLINWVGED	80-89	92
10	LREDENAEPV	50-59	26
11	SPSDSSTAST	339-348	63
12	LAASGEGGLQ	43-52	32
13	SESEVEEAAA	272-281	44
14	EESAADWALY	23-32	49
15	KSESEVEAA	271-280	20
16	ALDEVTSSQP	57-66	14
17	LELLAAYEEVIR	11-22	115
18	EDENAEPVGTTYQK	152-165	75
19	LREDENAEPVGTTYQK	150-165	18
20	LAASGEGGLQELSGHFENQK	43-62	65
21	SESEVEEAAAIIAQRPDNPR	272-291	37
22	ALDEVTSSQPPPPPPPPPPTQEAQE TTPSLDEE	357-389	145

Tab.3 List of 22 peptides (total score: 1212) with exact matches to drebrin, which were obtained by MALDI Q-TOF MS from the band of 120 kDa (see Fig.10).
(Score is $-10*Log (P)$, were P is the probability that the observed match is a random event. Individual ions score >50 indicate identity or extensive homology ($p<0,05$)).

5.4 Colocalization of drebrin and connexin43 at cell-cell contacts

Next the distribution of endogenous drebrin and connexin43 by immunofluorescence with corresponding antibodies was analysed. Immunofluorescence data from astrocytes and Vero cells clearly show that endogenous Cx43 is present at the Golgi region, non-contacting PM and at cell-cell contacts (Fig.10 a,b, Fig. 19 b). Endogenous drebrin is present inside the cells and at the PM. Intracellular drebrin localizes mostly along actin stress fibres in astrocytes (Fig.10c) and mostly at the Golgi region in Vero cells (Fig.19.a).

In astrocytes (Fig.10 b-d) and Vero cells (Fig.19 a,b) a clear colocalisation of both proteins underneath the plasma membrane in the regions of cell-cell contacts was observed. On the other hand, inside the cell and in non-contacting regions of the plasma membrane drebrin was not co-localised with Cx43 (Fig.10 d; Fig.19 a,b).
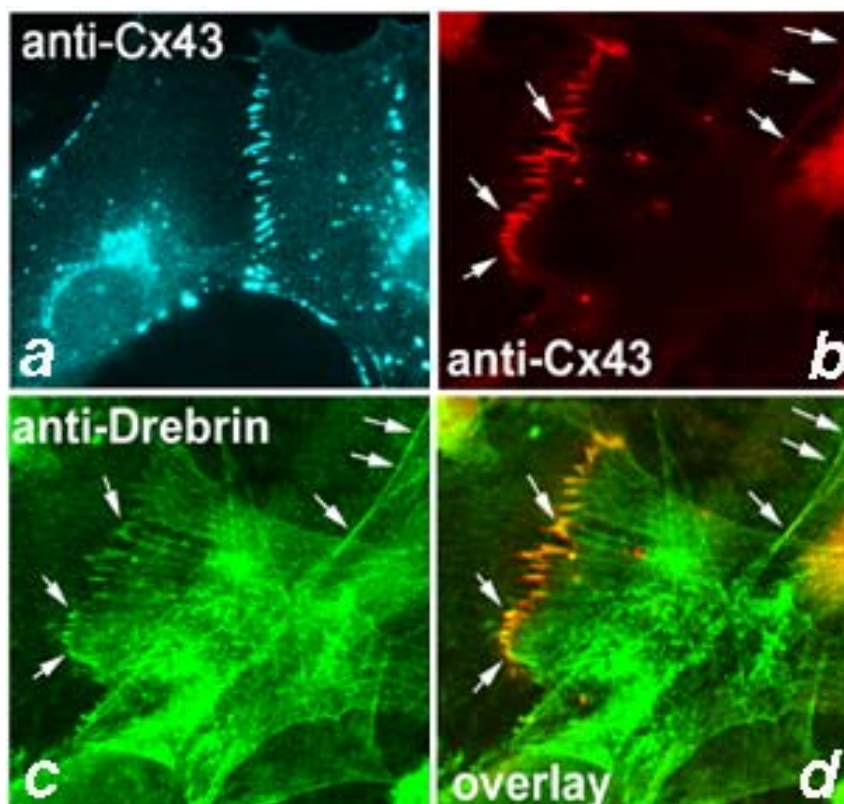

Fig.10 a): Distribution of endogenous connexin43 in mouse brain astrocytes
b,c,d): Colocalisation of endogenous drebrin and connexin43 at cell-cell contact in astrocytes as detected with anti-Cx43 and anti-drebrin M2F6 antibodies respectively.
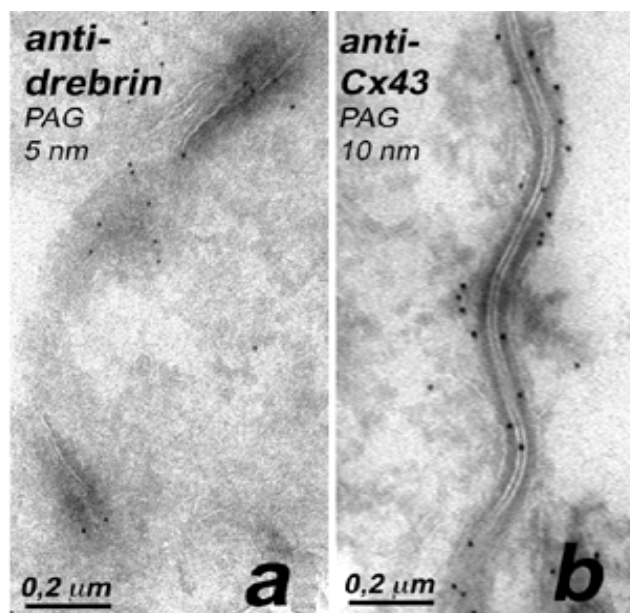
Fig.11 Distribution of CFP-drebrin (a) and Cx43-YFP (b) in Vero cells detected by immuno- electron microscopy. Note that in Vero cells (which have neither tight junctions, desmosomes or adherens junctions) drebrin is present in regions of cell-cell contact with a gap junction appearance.

5.5 Drebrin and connexin43 in subcellular fractions and immunoprecipitation using anti-Cx43 antibodies

Subcellular fractionation was performed to analyse the intracellular distribution of connexin43 and drebrin E.

Biotinylated plasma membrane fractions were identified by their reaction with streptavidin (Fig.12 a,b). Golgi fractions were identified with anti-ERD2 antibodies. ER fractions were detected using anti-KDEL-sequence antibodies (Fig.12 b).

The pellets of the plasma membrane, Golgi and ER fractions were analysed for the presence of drebrin and connexin. Drebrin was detected in the pellet of the plasma membrane fraction, but not in the pellet of Golgi fraction using anti-drebrin antibodies (Fig.12 c). Connexin43 was detected with anti-Cx43 antibodies preferentially in the pellet of both plasma membrane and Golgi fractions (Fig.12 d).

Immunoprecepitations using anti-Cx43 antibodies, raised against the first extracellular loop (residues 46 – 68) were performed with the fractions, and co-precipitating proteins

were analysed by immunoblotting with anti-drebrin antibodies. Drebrin was immunoprecipitated from the PM fraction (fraction1) but not from the Golgi fraction (fraction6) (Fig.12 e). These results confirm that drebrin is associated with Cx43 in the plasma membrane fraction.
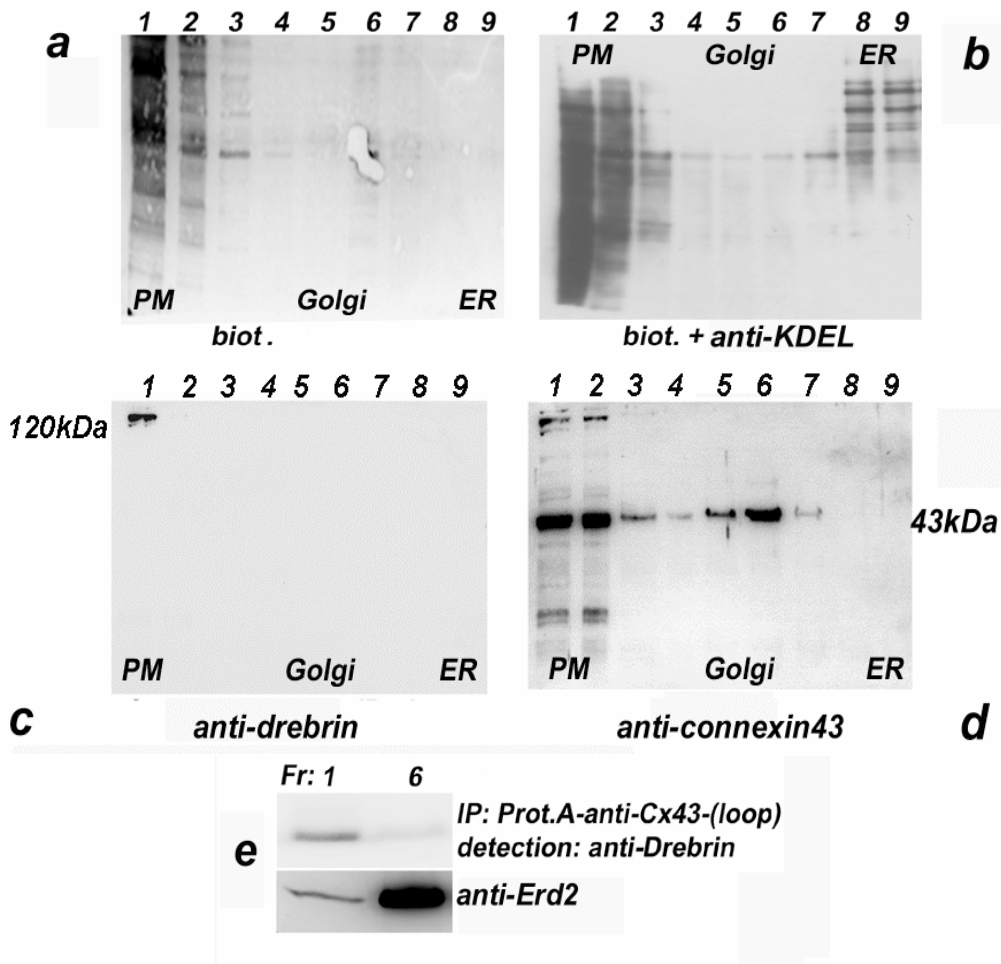

Fig. 12 Subcellular fractionation of Vero cells and characterisation of separated fractions.
a): Fractions containing biotinylated proteins, corresponding to the plasma membrane (PM) were detected with streptavidin-peroxidase.
b): Blot probed with streptavidin-peroxidase (fractions 1-3) was again exposed to anti-KDEL antibodies to reveal the endoplasmic reticulum (ER) proteins (fractions 8-9).
c): Drebrin was detected in the pellet of the plasma membrane fraction;
d): Connexin43 was present in the pellets of both plasma membrane and the Golgi fractions.
e): Anti-Cx43 antibodies immobilised on protein A sepharose can co-immunoprecipitate drebrin from the plasma membrane fraction (1) but not from the Golgi fraction (6). Anti-ERD2 antibodies (used as a control of the Golgi fractions) show the relative distribution of transmembrane Golgi protein in fractions 1 and 6.

5.6 Co-expression of fluorescent connexin43- and drebrin fusion proteins in Vero cells

Fluorescent fusion proteins of connexin43 and drebrin (CFP-drebrin and Cx43-YFP) were co-expressed in COS and Vero cells to investigate the intracellular distribution of these proteins. Live cell imaging revealed that drebrin is strongly accumulated in contacting regions of the plasma membrane only when Cx43 is present there (Fig.13; Fig.14 a,b; Fig.15 a-d).
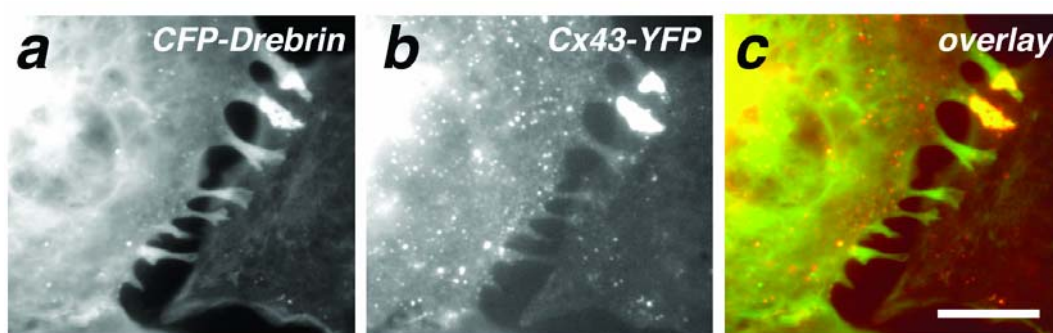

Fig.13 COS cells transfected with CFP-drebrin and Cx43-YFP plasmids reveal strong colocalisation of both proteins in the regions of cell-cell contacts. Note that overexpression of drebrin induces formation of processes (that was first described by Shirao et al., 1994), which form contacts with a neighbouring cell. Drebrin accumulates at zones of cell-cell contacts only if connexin43 is present there.

5.7 FRET analysis indicates CFP-drebrin/connexin43-YFP interaction in live Vero cells.

To confirm the close proximity of drebrin and connexin43 under the plasma membrane in the region of cell-cell contacts live cell fluorescence resonance energy transfer (FRET), using an acceptor bleach protocol (Majoul et al., 2001, 2002), was applied.

For these experiments CFP-drebrin and connexin43-YFP were expressed in Vero cells. In case of FRET proximity the photoinactivation of the acceptor (Cx43-YFP) results in an increase of the fluorescence of the donor (CFP-drebrin).

First, donor and acceptor images were acquired as follows: donor before bleach (Dbb), and acceptor before bleach (Abb) (Fig14 a,b; Fig.15 a-d). Acceptor inactivation was

performed in the region of cell-cell contact where both donor and acceptor were present, images were acquired as follows: acceptor after bleach (Aab) and donor after bleach (Dab) (Fig.14 c-d; Fig.15 e-f) and analysed using data processing (MetaMorph version 6.0 programm). The comparison of two graphs derived from the same cellular region obtained from the Dbb and Dab images revealed an increase of the donor fluorescence ranging from 15 to 25% (small arrows in zones of cell-cell contacts in (Fig.14 e; Fig.15 g). As a negative control the unchanged background region is depicted before and after the acceptor bleach (big arrows in Fig.14 e and Fig.15 g). The degree of acceptor photoinactivation in each pixel along the linescan is shown in Fig.14, e and Fig.15, g (Abb, Aab). 3D reconstruction of the profile scan (Fig.14 f; Fig.15 h) revealed the distribution of FRET between CFP-drebrin and Cx43-YFP underneath the plasma membrane.

FRET proximity between CFP-drebrin and connexin43-YFP was further confirmed in independent experiments using a Zeiss LSM510 META microscope setup (Fig.16). CFP-drebrin and Cx43-YFP interactions were analysed in live cells during the time-dependent photoinactivation of the acceptor in the region of cell-cell contacts were both donor and acceptor were present (Fig.16 a). The time-dependent increase in the donor fluorescence (CFP-drebrin) was inversely proportional to the degree of acceptor (Cx43-YFP) inactivation (Fig.16 b). All images are representative of at least 3 independent sets of experiments and confirm that the interaction between drebrin and connexin43 occurs in a live cell in the region of cell-cell contact.
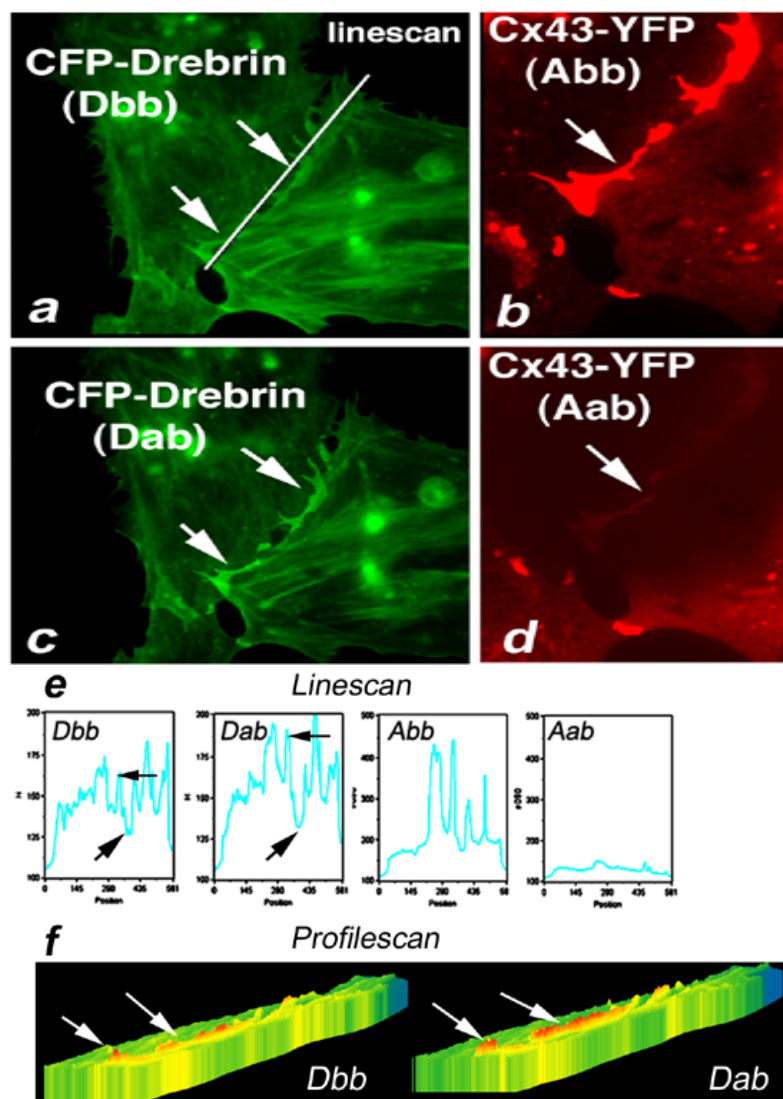
Fig. 14 FRET analyses of live Vero cells, expressing CFP-drebrin (donor)/connexin43-YFP (acceptor).

a - b): Donor (Dbb) and acceptor (Abb) images before acceptor bleaching.

c - d): Donor (Dab) and acceptor (Aab) images after acceptor bleaching by laser irradiation at λ_{ex} =530 nm.

e): corresponding linescans (Dbb, Dab, Abb, Aab) along cell-cell interface: small arrows indicate increase in donor fluorescence, big arrows show unchanged background.

f): 3D reconstruction of profile scan shows the distribution of FRET between CFP-drebrin and Cx43-YFP under the plasma membrane (arrows indicate increase in donor fluorescence of Dab compared to Dbb).
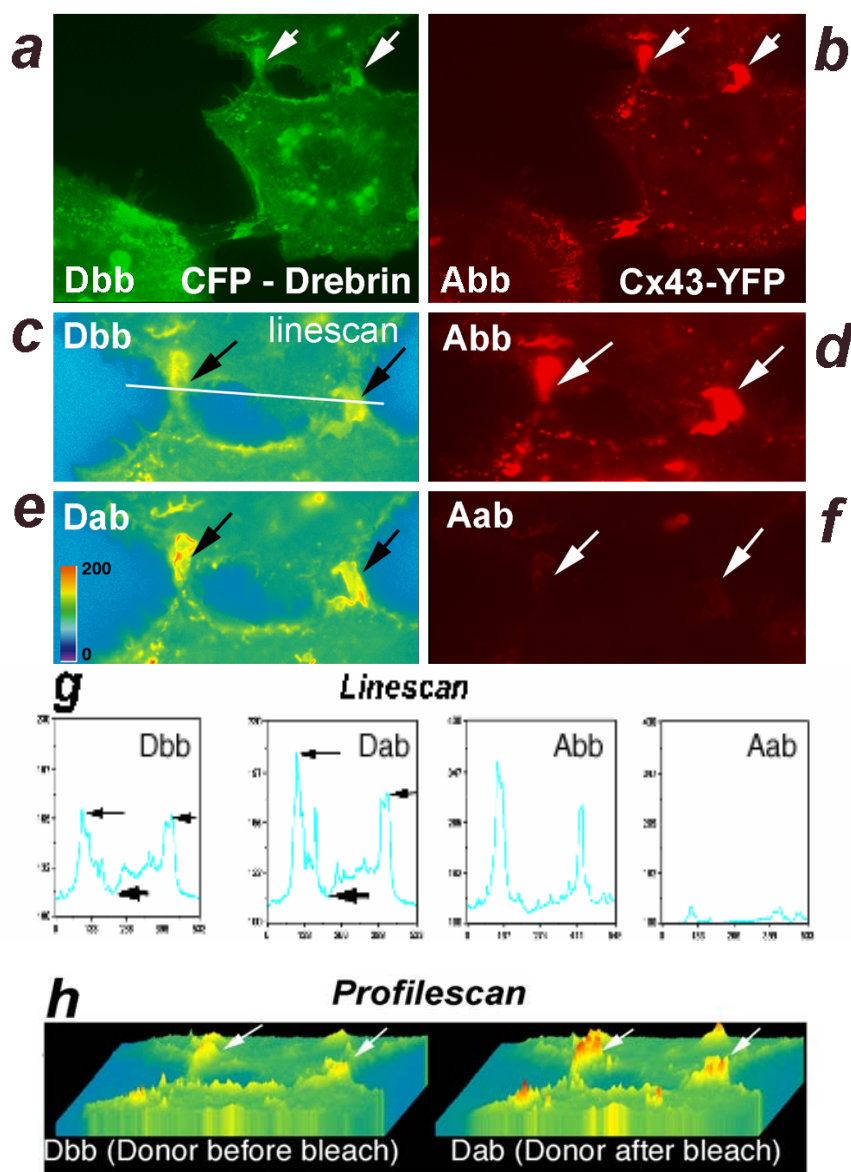
Fig.15 FRET analyses of live Vero cells, expressing CFP-drebrin/connexin43-YFP.
a –b):CFP-drebrin (donor) and Cx43-YFP(acceptor), expressed in Vero cells, colocalise at cell-cell contact (arrows).
c - d): Donor (Dbb) and acceptor (Abb) images before acceptor bleaching
e - f): Donor (Dab) and acceptor (Aab) images after acceptor bleaching by laser irradiation at λ_{ex} 530 nm.
g): corresponding linescans (Dbb, Dab, Abb, Aab) along cell-cell interface: small arrows indicate increase in donor fluorescence, big arrows show unchanged background.
h): 3D reconstruction of profile scan shows the distribution of FRET between CFP-drebrin and Cx43-YFP under the plasma membrane (arrows indicate increase in donor fluorescence of Dab compared to Dbb).
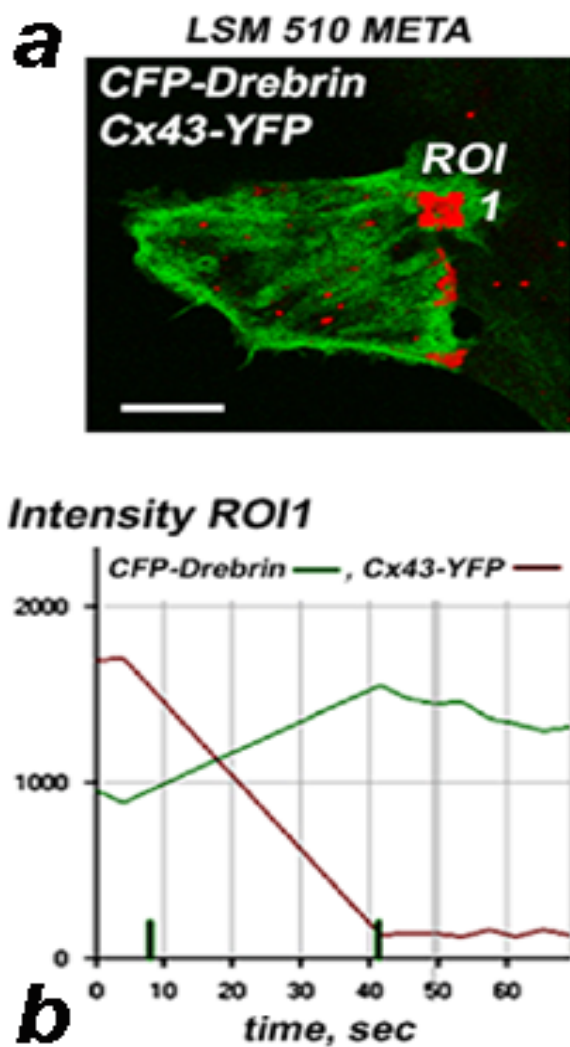
Fig.16 FRET between CFP-drebrin and Cx43-YFP detected with the LSM 510 Meta microscope.

a): Pair of Vero cells expressing CFP-drebrin (donor), shown in green and Cx43-YFP (acceptor), shown in red, before inactivation of acceptor.

Laser irradiation λ_{ex} 514 nm was applied to bleach Cx43-YFP (acceptor) in the region of cell-cell contact ROI1

b): Registration of intensity of donor and acceptor fluorescence during bleaching of acceptor. Time-dependent increase in the donor fluorescence (CFP-drebrin) is inversely proportional to the degree of acceptor (Cx43-YFP) inactivation.

5.8 Analysis of connexin43-drebrin interaction by si-RNA induced drebrin depletion

To understand the role of an interaction between drebrin and connexin43 in a live cell the level of endogenous drebrin was reduced by transfection with si-RNA duplex oligos directed against drebrin m-RNA.

In control Vero cells drebrin and Cx43 were colocalized at the regions of cell-cell contacts as was detected by immunofluorescence (Fig.19 a,b). 48 h after oligofectamine transfection with the si-RNA oligos against drebrin a significant decrease in both the immunoblot (Fig.17) and immunofluorescence signals with anti-drebrin antibodies (Fig.19 c) was observed.

The decrease in the endogenous drebrin level in si-RNA transfected Vero cells resulted also in a dramatic decrease of the endogenous Cx43 level compared to the control cells (Fig.17; Fig.19 d). Moreover, in astrocytes drebrin depletion by si-RNA correlated with loss of phosphorylated Cx43 forms (Fig.18).

A si-RNA knock-down of drebrin increased connexin43-GFP scattering through the cytoplasm (Fig.20 a) as compared to the membrane appearance in control cells. Electron microscopy analysis of these cells revealed the formation of multimembrane structures corresponding to internalised "annular junctions" (Fig.21).

Furthermore, in actin-GFP expressing cells we observed extensive ruffling of the plasma membrane after transfection with drebrin-siRNA that was not observed in control cells (Fig.22).
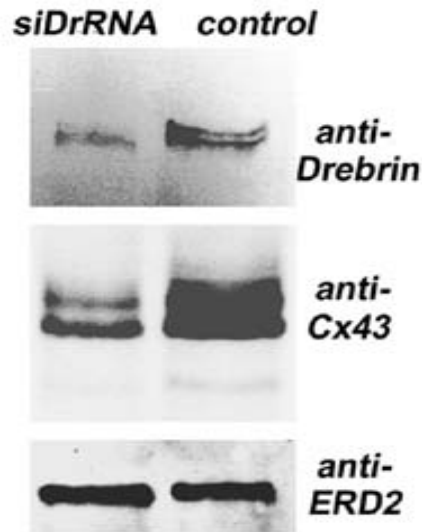
Fig.17 Immunoblot analysis of Vero cells transfected with siRNA directed against drebrin (24 h after transfection). Note that the decrease in drebrin level results in a dramatic decrease of Cx43 level compared to the control cells. Anti-ERD2 antibodies were used as a loading control.
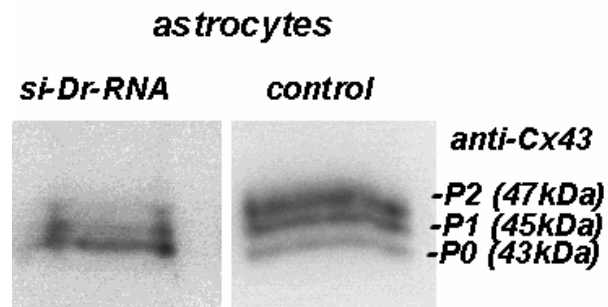

Fig.18 Western blot of astrocytes transfected with siRNA against drebrin and stained with anti-connexin43 antibodies (24h after transfection). Si-RNA–transfected astrocytes show not only a decrease of total connexin43 but also a shift from the phosphorylated forms to the nonphosphorylated species.
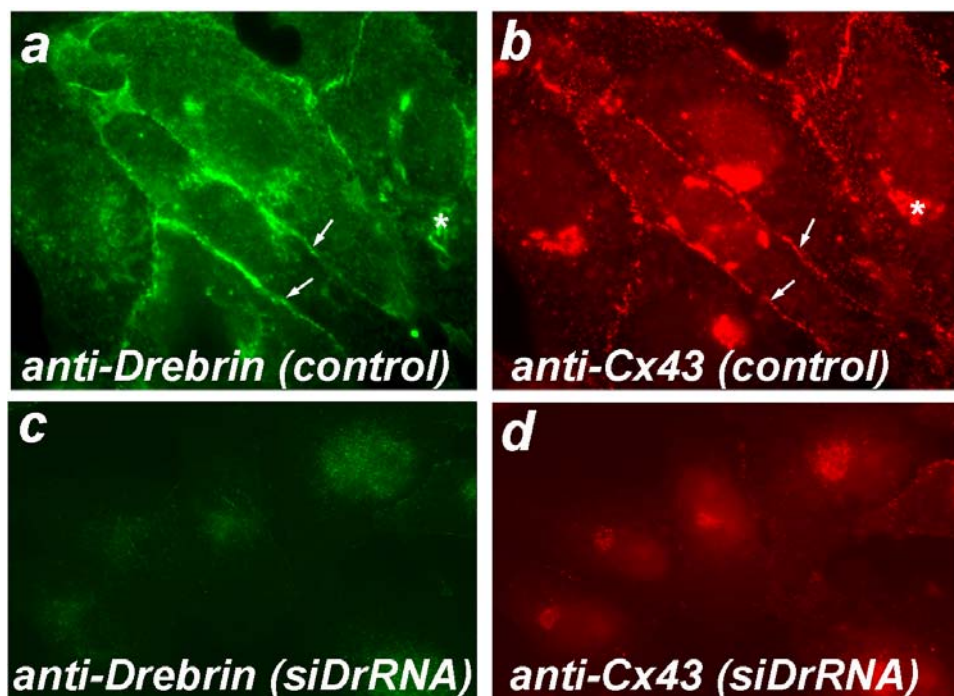
Fig.19 a-b): Distribution of endogenous drebrin and connexin43 in Vero cells revealed by immunofluorescence with anti-drebrin and anti-Cx43 antibodies. Both proteins colocalize under the plasma membrane (arrows) but do not colocalize in the Golgi region (*).
c – d): Localization of drebrin and Cx43 detected 48h after transfection of Vero cells with si-RNA against drebrin as detected with the same antibodies. Note that decrease in the level of drebrin correlates with a decrease of Cx43 immunoreactivity and disappearance of Cx43 from the submembrane zones of cell-cell contacts.
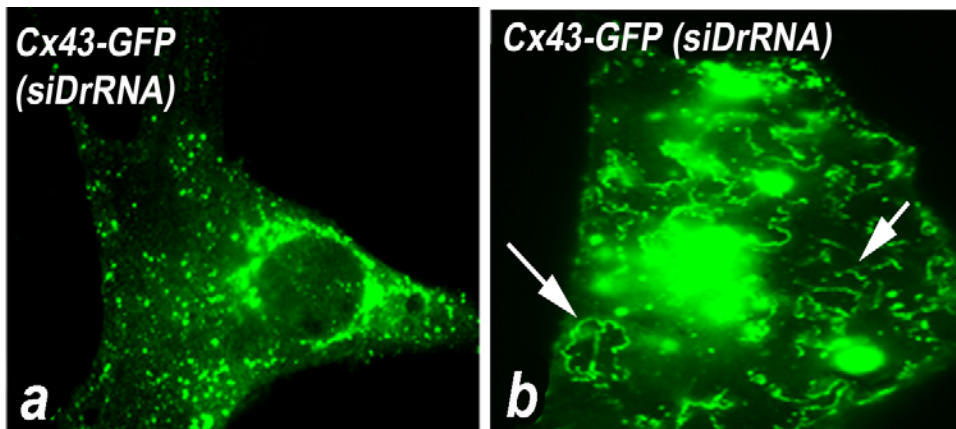
Fig.20 a): Scattering of Cx43-GFP through out the cytoplasm in Vero cells transfected first with siRNA against drebrin (24h) followed by Cx43-GFP plasmid transfection (10h). b):Vero cells co-transfected with siRNA against drebrin and a plasmid coding for Cx43-GFP (10h). Arrows show the ruffled lesions of the plasma membrane.

Fig.21 Immuno electron microscopy of Vero cells co-transfected with Cx43-GFP and si-RNA against drebrin and stained with anti-Cx43 antibodies (10h after transfection). Arrows indicates the formation of multimembrane "annular junctions".
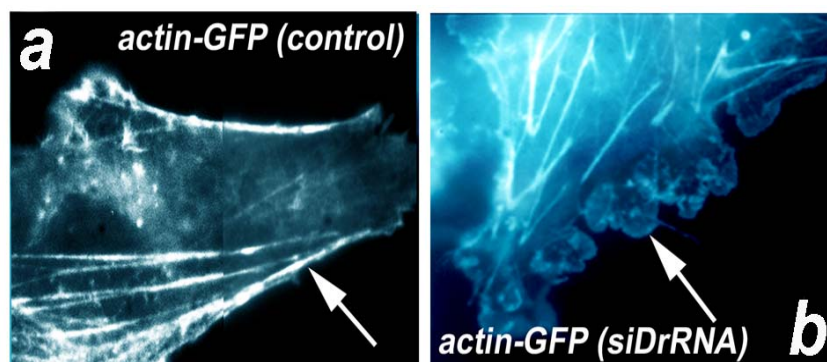
Fig.22 Vero cells transfected with a plasmid coding for GFP-actin (a) or co-transfected with si-RNA against drebrin and a plasmid coding for GFP-actin (b). Down-regulation of drebrin induces a dramatic ruffling of the plasma membrane (shown 10 h after transfection).

5.9 Effect of latrunculin B on a state of drebrin

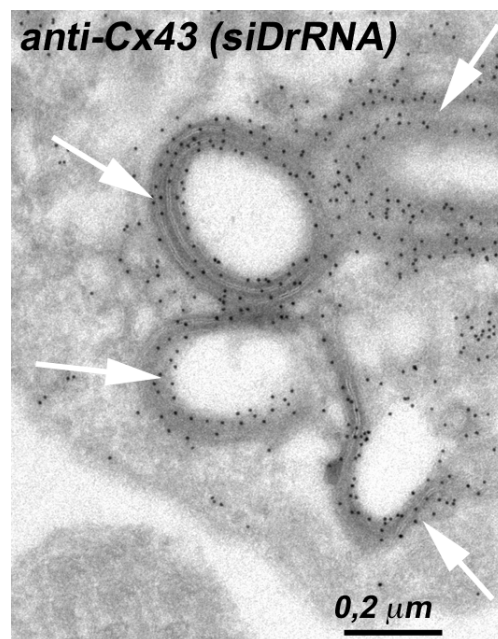To test whether the submembrane localization of drebrin depends on the presence of polymerized actin, we treated Vero cells with the actin- depolymerising drug, latrunculin B (100nM). In Vero cells, co-expressing connexin-YFP and CFP-drebrin, drebrin accumulated underneath the plasma membrane of contacting cells after latrunculin B treatment, i.e was not dispersed through the cytoplasm in the absence of actin filaments (Fig.23).

Fig.23 Time dependent accumulation of drebrin under the plasma membrane of Vero cells coexpressing CFP-drebrin and Cx43-YFP upon latrunculin B treatment.

5.10 Functional analyses of connexin43-drebrin interaction

Dye transfer analysis and electrical coupling experiments were applied to analyse the functional state of gap junctions at decreased levels of drebrin following treatment with anti-drebrin si-RNA.

5.10.1 Dye transfer analysis

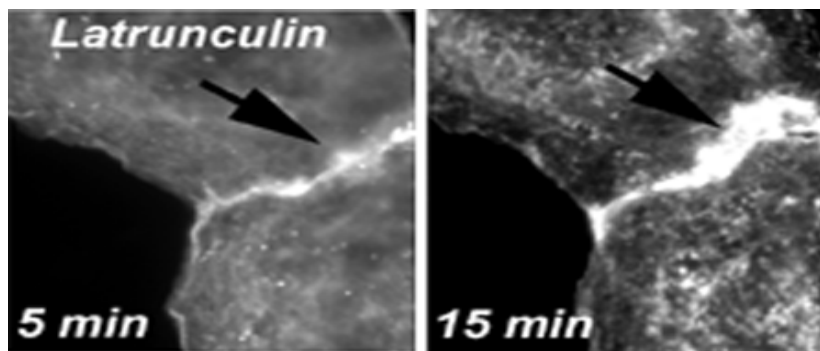Astrocytes of confluent monolayer, non-transfected or transfected with si-RNA against drebrin were microinjected with calcein. In control cells, dye was immediately transferred from one cell to 8-20 neighbouring (n=10). Transfer of calcein between drebrin-deficient astrocytes was slower and was visible in only 2-3 neighbouring cells (n=12) (Fig.24).
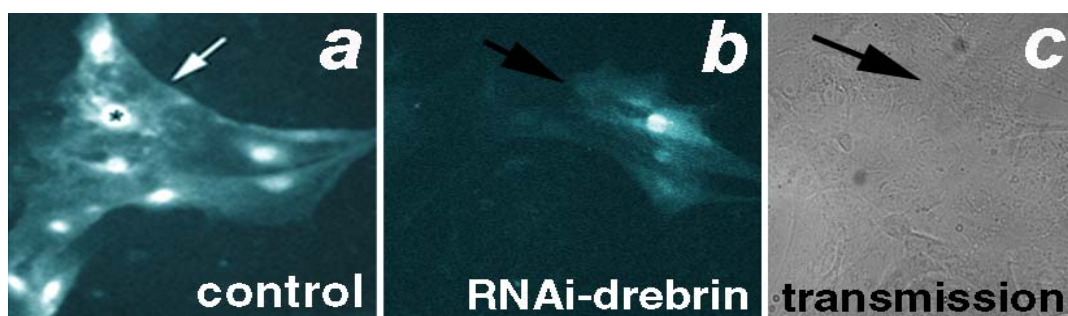
Fig.24 a): Astrocytes microinjected with calcein display within a few seconds the transfer of dye to the adjacent cells via the functional gap junctions (* indicates a microinjected cell). b-c): Strong decrease of calcein transfer observed in astrocytes transfected with drebrin si-RNA (24 h after transfection), although contacting cells are clearly visible in the transmission light image.

5.10.2 Electrical coupling experiments

Double whole-cell voltage-clamp recording of pairs of primary cultured astrocytes was used to analyse the state of cell-cell contact permeability (Fig.25). One cell of the pair was exposed to voltage pulses of 200 ms with a holding potential at -70 mV/ 10 mV increment (cell1), wile the adjacent cell was kept at −70 mV (cell2). Current responses from both cells, the stimulated cell (I_1) and the neighbouring cell coupled through the gap junctions (I_2) were recorded.

Comparison of the currents that pass through the gap junctions (I_2) of control cells, of cells co-transfected with drebrin-si-RNA and a plasmid encoding the transmembrane Golgi protein p23-CFP, or control cells transfected with just the p23-CFP plasmid revealed a strong decrease in cell-cell permeability in drebrin si-RNA transfected astrocytes (Fig.25). This effect was statistically significant indicating that si-RNA-mediated depletion of drebrin strongly decreases cell-cell permeability.
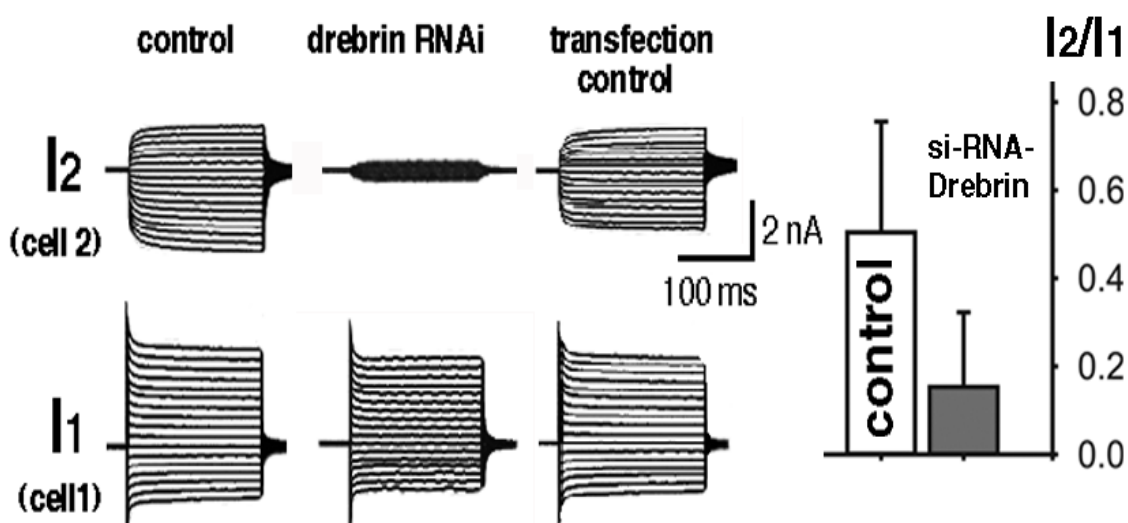
Fig.25 Double whole cell voltage clamp recordings of a pair of cultured protoplasmic astrocytes. One cell of the pair (cell 1) was exposed to voltage pulses (200ms; holding potential – 70mV; 10mV increment), while adjacent cell (cell 2) was kept at –70mV. Currents from the stimulated cell (I_1) and currents that pass through the gap junctions (I_2) were recorded from either control cells, cells co-transfected with si-RNA against drebrin plus a control plasmid encoding the transmembrane Golgi protein p23-CFP, or cells transfected with the p23-CFP plasmid alone. Cells transfected with si-RNA against drebrin were recognized by the p23-CFP signal and by Cy3 label of the oligos. Three representative cells are shown together with a statistical evaluation (n=5 for control cells and n=6 for cells transfected with drebrin si-RNA). Control astrocytes: coupling ratio = I_2 / I_1 = 0.52+/-0.27; si-RNA drebrin: I_2 / I_1 = 0.14 +/- 0.03 (n=5), P<0.004.

6. Discussion

Connexins form gap junctions that mediate the transfer of ions, metabolites and second messengers between contacting cells. Many connexin functions, e.g cellular transport, plaque assembly and stability, and channel conductivity are finally tuned and most likely involve proteins that bind to the cytoplasmic domains of connexins. However, little is known yet about such regulatory proteins.

In the present work new proteins, which are involved in the intracellular trafficking of connexin43 and in the maintenance of the functional activity of gap junctions underneath the plasma membrane were identified.

Plasma membrane appearance of connexin43 was found to depend on the functional activity of the small-GTPases Sar1 and ARF1. Transport of Cx43 from the ER to the Golgi apparatus was blocked by expression of a GTP-restricted mutant of Sar1. GTP-bound mutant of ARF1 prevented transport of Cx43 from the Golgi apparatus to the plasma membrane.

Drebrin was identified by a proteomics approach as a new interacting partner for the COOH-terminal domain of connexin43. Drebrin had previously been described as an actin-binding protein that is decreased in brains during Alzheimer's disease progression. The novel drebrin-Cx43 interaction described in my work was confirmed by colocalisation of endogenous proteins in astrocytes and in Vero cells, co-immunoprecipitation, electron microscopy, electrophysiology, co-expression of both proteins with fluorescent tags and by live cell FRET analysis. Depletion of drebrin in cells with si-RNA resulted in impaired dye and electrical coupling, internalisation of gap junctions, and targeting of Cx43 to a degradative pathway.

6.1 Involvement of small GTPases in the intracellular trafficking of connexin43

Intracellular trafficking of connexins is an area of intense interest, since mutations in plasma membrane proteins, that inhibit their transport to the cell surface, can cause diseases (Kim and Arvan, 1998; Aridor and Balch, 1999). Such diseases result from the absence of the wild-type protein and proteins associated with it, from the plasma

membrane. In some cases undegraded proteins accumulate in the ER and induce chronic endoplasmic reticulum stress response, which in turn can lead to major changes in cell physiology such as in the case of a mutant of connexin32, which causes Charcot-Marie-Tooth peripheral neuropathy (Deschenes et al., 1997).

Connexin43, as many other plasma membrane proteins, pass from the ER through the Golgi apparatus to the plasma membrane. Nevertheless, the details of intracellular trafficking of connexin43 from the ER as well as data about the involvement of the COPII and COPI-dependent machineries in this process are unknown.

The small GTPase Sar1 is involved in the COPII-dependent budding of transport vesicles from the ER membrane (Yoshihisa et al., 1993; Kuge et al., 1994; Aridor et al., 1995, 2001). The exchange of GDP for GTP activates Sar1, causes it to bind to the ER membrane and induce the recruitment of coat proteins to form coated buds and subsequently coated vesicles. Expression of a GTP-restricted mutant Sar1 in Vero cells blocks the formation of COPII coated transport vesicles and subsequently the trafficking of Cx43 from the ER. Moreover, connexin43 accumulates in the ER release sites, co-localising with Sec13p, a protein of the COPII complex, which is considered to be a marker of ER-release sites (Salama et al., 1993; Hobman et al., 1998; Tang et al., 1997). ARF1 (ADP-ribosylation factor) is a small GTPase, which regulates the budding of COPI coated transport vesicles from the Golgi network (Pepperkok et al., 1998; Schekman and Orci, 1996; Springer et al., 1999; Sprang et al., 2002). ARF1Q71L, a GTP-restricted mutant of ARF1, which is bound to the Golgi membrane, induces accumulation of Cx43 in the Golgi complex.

These findings suggest that transport of connexin43 to the plasma membrane is dependent on the functional activity of small GTPases Sar1 and ARF1 and thus COPII and COPI-mediated processes. Disturbance of anterograde trafficking to the plasma membrane induces accumulation of connexin43 inside the ER or the Golgi complex.
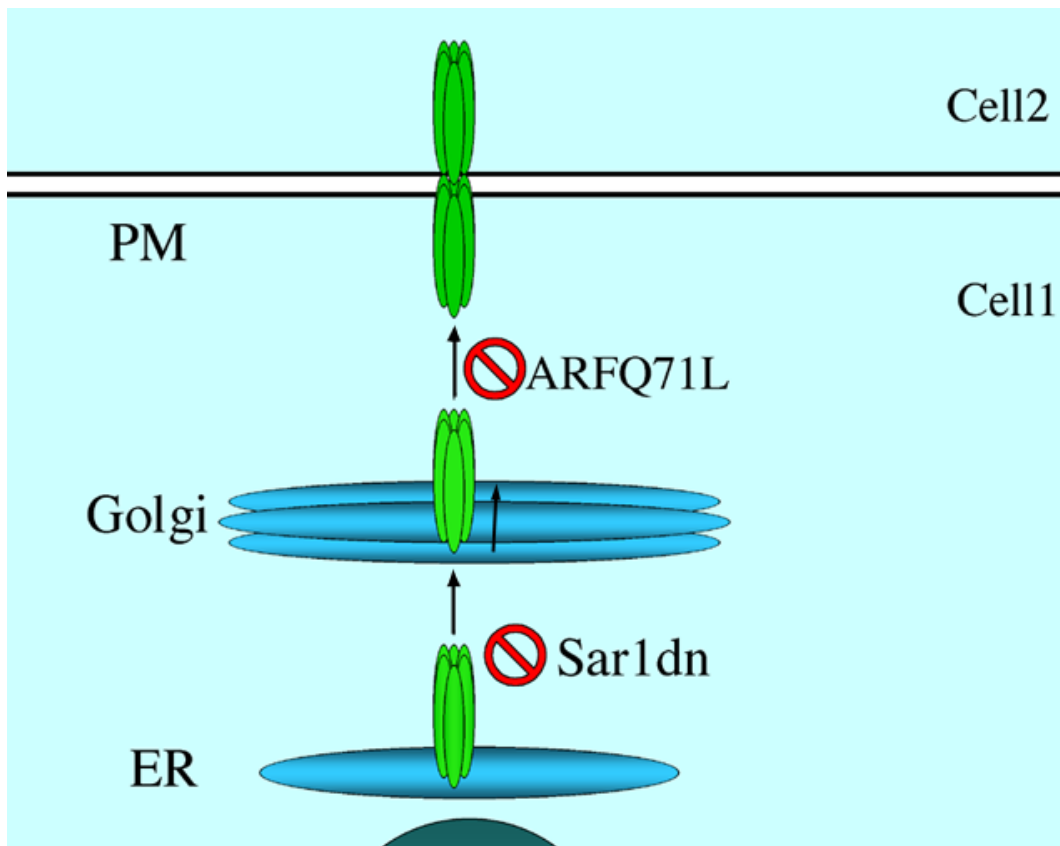
Fig.26 Transport of connexin43 to the plasma membrane can be blocked by GTP-restricted GTPases Sar1dn or ARF1Q71L. Expression of Sar1 dn blocks exit of Cx43 from the ER, ARF1Q71L induces accumulation of Cx43 in the Golgi.

6.2 Identification of proteins interacting with connexin43

Potentially, the cytoplasmic C-terminal domain of Cx43 is a highly regulated region that contains multiple sequences for interactions including modification by phosphorylation by different kinases and molecules that will recognize the phosporylated C-terminus, tubulin, ZO-1, and other molecules containing PDZ, SH2, and SH3 domains.

In search for new interaction partners of Cx43 a proteomics approach was used to screen subcellular fractions from different mouse tissues (brain, kidney, lung, heart, liver) for proteins that may interact with a GST-fusion protein encompassing the COOH-terminal domain of Cx43 (residues 234-382), which is exposed to the cytosol.

Pull-down assay using this Cx43-COOH terminal domain fusion protein recovered several bands that were resolved by SDS-PAGE and visualized with Coomassie Blue. MALDI/ Q-TOF (matrix assisted laser desorption ionisation/ quadripole time of flight) mass spectrometry analysis of tryptic peptides identified a number of these proteins. One of them, drebrin E, was reproducibly recovered in pull-down assays from the brain membrane fraction using the Cx43-GST fusion protein. 22 matching peptides with exact matches to cDNA-derived protein sequence of drebrin were obtained by Q-TOF sequence analysis.

A 55 kDa band was identified as β-tubulin, which had already been described as a protein interacting with Cx43 (Giepmans et al., 2001). Another previously described Cx43 interacting protein, the tight junction protein ZO-1 (Toyofuku et al., 1998; Giepmans and Moolenaar, 1998), was not recovered on the Cx43-GST fusion protein under our experimental conditions, which included the presence of 1% Triton and ATP in the binding reaction and wash buffers.

6.3 Interaction between connexin43 and drebrin

As an interaction between connexins and drebrin had not been described before, I put the main emphasise of my work on this aspect.

Drebrin is an F-actin- binding protein originally identified in brain as a neuronal-specific **d**evelopmentally **re**gulated **br**ain prote**in** (Shirao and Obata, 1985; Ishikawa et al., 1994). Drebrin exists in two isoforms: A (adult) and E (embryonic). Drebrin A is specifically located in the postsynaptic dendritic spines of neurons (Hayashi et al., 1996) and involved in their plasticity (Hayshi and Shirao, 1999). Drebrin E is a ubiquitous isoform, which localises to the submembrane region of neurons as well as non-neuronal cells such as stomach and kidney epithelia (Asada et al., 1994; Keon et al., 2000). Recently it has been shown that drebrin regulates interactions between the NR1 subunit of the NMDA glutamate receptor and α-actinin, calmodulin and actin filaments (Shirao and Sekino, 2001).

Drebrin contains an actin-depolymerizing factor (ADF-H) domain and at least one SH3-domain of five prolin-rich domains (Lappalainenen al., 1998; Larbolette et al., 1999). SH3-domains are 50-70 amino acid long protein domains that bind to the GK

(guanylate kinase- homologous) module or to proteins containing a PXXP sequence. It may be of importance, that the COOH terminus of connexin43 contains PXXP domains, which could bind to the SH3-domain of drebrin.

6.4 Drebrin - connexin43 interaction occurs under the plasma membrane of contacting cells

Immunostaining with corresponding antibodies revealed that in astrocytes and in Vero cells drebrin and connexin43 clearly co-localise underneath the plasma membrane in the region of cell-cell contacts. In contrast, around the Golgi region both proteins are also present but clearly segregated from each other. Co-expression of CFP-drebrin and Cx43-YFP constructs in live COS cells revealed that drebrin is strongly accumulated in contacting regions of the plasma membrane only if Cx43 is present there. FRET analysis (acceptor bleach) revealed significant increase of the donor (CFP-drebrin) fluorescence after bleaching of the acceptor (Cx43-YFP) indicating the close proximity of CFP-drebrin and connexin43-YFP under the plasma membrane of contacting cells. In vitro drebrin can be co-immunoprecipitated with connexin43 from the plasma membrane fraction, but not from a Golgi membrane fraction.

Taken together, this indicates that the interaction of connexin43 and drebrin is specific for the plasma membrane and does not occur around the Golgi region.

6.5 Drebrin may facilitate formation of gap junctions by alignment of the plasma membranes of contacting cells

CFP-drebrin and GFP-actin expressed in Vero cells are co-localised both at the plasma membrane and at stress fibres. An interesting finding was made in experiments following depletion of drebrin. Transfection of cells with si-RNA directed against drebrin affected only actin, localised at the plasma membrane, but not actin stress fibres, and induced dramatic ruffling of the plasma membrane, which was not observed in control cells.

These findings suggest that drebrin-actin interaction under the plasma membrane is important to preserve the cell shape and that alignment of the contacting plasma membranes is a necessary condition for gap junction formation.

6.6 Interaction between drebrin and connexin at gap junctions is stronger than interaction between drebrin and actin

Treatment of Vero cells with the actin-depolymerising drug latrunculin B resulted in accumulation of drebrin underneath the plasma membrane of contacting cells and thus drebrin was not dispersed through the cytoplasm in the absence of actin filaments.

These data indicate that the interaction between drebrin and connexin43 under the plasma membrane is much stronger that between drebrin and actin and are in agreement with data from Ikeda and colleagues (1996) and Peitsch and colleagues (1999), who showed that drebrin-positive plaques, localised at cell-cell contacts, are resistant to cytochalasin D.

6.7 Drebrin is required for the functional activity of gap junctions between contacting cells

It was shown previously that depolymerisation of F-actin by cytochalasins as well as microinjection of anti-actin antibodies lead to the reduction of dye transfer, electrical coupling and propagation of calcium waves via gap junctions (Branes et al., 2002, Theiss and Meller, 2002; Cotrina et al., 1998).

Here, the role of drebrin in the maintenance of the functional activity of gap junctions was analyzed. Depletion of drebrin level by si-RNA transfection resulted in 80 % decrease of dye transfer between adjacent cells. Protoplasmic astrocytes, which are normally strongly electrical coupled, showed a dramatic decrease (64 %) of the coupling ratio after drebrin knock-down. These data prove the importance of the drebrin-connexin43 interaction for the maintenance of functional activity of gap junctions.

6.8 Drebrin keeps the phosphorylated forms of connexin43 at the plasma membrane

Connexin43 is a protein that known to be phosphorylated on both serine and tyrosine residues, which changes its mobility upon SDS-PAGE (Lin et al., 2001; Ten Broek et al., 2001; Faucheux et al., 2004). Normally, in immunoblots of cultured mouse astrocytes the

anti-Cx43 antibodies show predominantly the upper, phosphorylated bands of Cx43. Recently, Faucheux and co-workers (2004) using inhibitors of cAMP-dependent protein kinase and protein kinase C showed a correlation between disappearance of Cx43 phosphorylated bands and a strong decrease in gap junction permeability. Similarly, in my experiments, siRNA-mediated drebrin depletion in astrocytes induced a reduction of the phosphorylated P1 and P2 bands of Cx43 together with a reduction of dye- and electrical coupling. Therefore it is tempting to speculate that drebrin in astrocytes (most likely together with other submembrane proteins) may favor the functional stabilization of Cx43 at the plasma membrane.

6.9 Stabilization of gap junctions under the plasma membrane by drebrin prevents its degradation

My experiments indicate that the abolishment of the interaction between connexin43 and drebrin under the plasma membrane is responsible for the removal of gap junctions from the plasma membrane and targeting of Cx43 to a degradative pathway.
The decrease in the endogenous drebrin level induced by transfection of cells with si-RNA against drebrin resulted in a dramatic decrease of the endogenous Cx43 level. Transfection with drebrin-si-RNA induced the scattering of Cx43-GFP through out the cytoplasm and in a perinuclear Golgi region and prevented appearance of Cx43-GFP in regions of cell-cell interface. Immuno-electron microscopy of these cells revealed a large amount of "annular junctions", which represent internalised gap junctions.

6.10 Drebrin may serve to convey signals from the connexin43 to intracellular effectors

In the present work it has been demonstrated that drebrin interacts with the COOH-terminal domain of Cx43 and is required to maintain functional gap junctions in Vero cells and in astrocytes.

Initially, drebrin was described as an actin binding protein (Asada et al., 1994; Ishikawa et al., 1994). Drebrin thus may functions as a linker between gap junctions and the actin sub-membrane cytoskeleton. Indeed, a scaffolding role of drebrin in the

submembrane cytoskeleton of dendritic spines has already been documented (Shirao and Sekino, 2001).

Precedents for the regulation and stabilisation of cell-cell contacts via crucial interactions with cytoplasmic proteins are well known (Jamora and Fuchs, 2002). In the classical adherence junctions, E-cadherin conveys signals to intracellular effectors using α− and β− catenins to modify the submembrane cytoskeleton in response to extracellular stimuli. Similarly, drebrin may act as adapter protein that links connexin43 / gap junction signalling to the submembrane cytoskeleton.
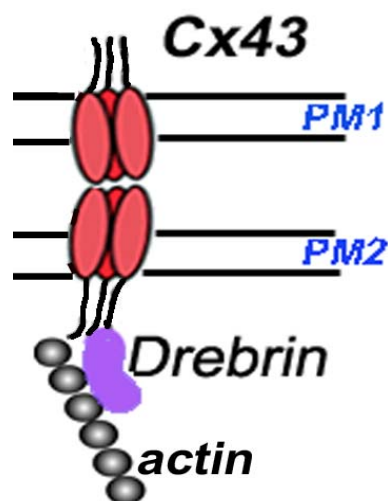
Fig. 27 Proposed model for Cx43/drebrin/actin interactions. Drebrin can act as an adaptor protein that links connexin43/gap junction signalling to components of the actin cytoskeleton.

6.11 Connexin dysfunction may be responsible for the memory loss in Alzheimer's disease

Alzheimer's disease (AD) is the most common cause of dementia in the elderly, which cause progressive defects in memory, cognition, attention and motivation. Pathogenesis of AD involves alteration in ion channels, PKC, calcium homeostasis, amyloid processing and extensive synapse loss (Hensley et al., 1994; Chan et al., 2002; Lim et al., 2003; Stutzmann et al., 2004).

Recent data indicates, that AD is associated with an 81% decrease in levels of drebrin, which regulates postsynaptic plasticity (Harigaya et al., 1996; Hatanpaa et al., 1999; Shim and Lubec, 2002).

My experiments with siRNA depletion of drebrin may mimic the decreased level of drebrin in AD that will cause an increased degradation of gap junctions and as a consequence impairment of electrical transmission.

To test the hypothesis of drebrin/connexin involvement in AD more experiments need to be designed and performed in whole animal experiments.

7. Conclusions

In the present work I showed for the first time that transport of connexin43 from the ER to the plasma membrane is dependent on the activity of small GTPases Sar1 and ARF1 and thus COPII and COPI-mediated processes.

Drebrin, an actin-binding protein, has been identified by proteomcs approach as a new interacting partner for COOH-terminal domain of Cx43. The novel connexin43-drebrin interaction was confirmed by colocalization of endogenous proteins in astrocytes and in Vero cells, co-immunoprecipitation, electrophysiology, co-expression of both proteins with fluorescent tags and by live cell FRET analysis. Depletion of drebrin in cells with si-RNA resulted in internalization of gap junctions and impaired cell-cell coupling.

On the basis of these data I conclude that drebrin is required to maintain Cx43-containing gap junctions in their functional state at the plasma membrane. It is thus possible that drebrin may interact with gap junctions in zones of cell-cell contacts in a regulated fashion in response to extracellular signals. The rearrangement or disruption of interaction between connexin43 and the drebrin-containing submembrane cytoskeleton directs connexin43 to degradative cellular pathways.

References:

Aberle H, Schwartz H, Kemler R. (1996)
Cadherin-catenin complex: protein interactions and their implications for cadherin function.
J Cell Biochem. 61, 514-23.

Allbritton NL, Meyer T, Stryer L. (1992)
Range of messenger action of calcium ion and inositol 1,4,5-trisphosphate.
Science. 258:1812-5.

Aridor M, Balch WE. (1999)
Integration of endoplasmic reticulum signaling in health and disease.
Nat Med. 5, 745-51.

Asada H, Uyemura K, Shirao T. (1994)
Actin-binding protein, drebrin, accumulates in submembranous regions in parallel with neuronal differentiation.
J Neurosci Res. 38, 149-59.

Berridge MJ, Irvine RF. (1989)
Inositol phosphates and cell signalling.
Nature. 341, 197-205.

Berridge MJ. (1997)
Elementary and global aspects of calcium signalling.
J Physiol. 499, 291-306.

Beyer EC, Paul DL, Goodenough DA. (1990)
Connexin family of gap junction proteins.
J Membr Biol. 116, 187-94.

Beyer EC, Gemel J, Martinez A, Berthoud VM, Valiunas V, Moreno AP, Brink PR. (2001)
Heteromeric mixing of connexins: compatibility of partners and functional consequences.
Cell Commun Adhes. 8, 199-204.

Bjorkman N. A study of the infrastructure of the granulosa cells of the rat ovary. (1962)
Acta Anat. 51, 125-147

Boitano S, Dirksen ER, Sanderson MJ. (1992)
Intercellular propagation of calcium waves mediated by inositol trisphosphate.
Science. 258, 292-5.

Boitano S, Dirksen ER, Evans WH. (1998)

Sequence-specific antibodies to connexins block intercellular calcium signaling through gap junctions.
Cell Calcium. 23, 1-9.

Chan SL, Furukawa K, Mattson MP. (2002)
Presenilins and APP in neuritic and synaptic plasticity: implications for the pathogenesis of Alzheimer's disease.
Neuromolecular Med. 2, 167-96.

Cheng HL, Louis CF. (2001)
Functional effects of casein kinase I-catalyzed phosphorylation on lens cell-to-cell coupling.
J Membr Biol. 181, 21-30.

Cooper CD, Lampe PD. (2002)
Casein kinase 1 regulates connexin-43 gap junction assembly.
J Biol Chem. 277, 44962-8

Cotrina ML, Lin JH, Nedergaard M. (1998)
Cytoskeletal assembly and ATP release regulate astrocytic calcium signaling.
J Neurosci. 18, 8794-804.

Crow DS, Beyer EC, Paul DL, Kobe SS, Lau AF. (1990)
Phosphorylation of connexin43 gap junction protein in uninfected and Rous sarcoma virus-transformed mammalian fibroblasts.
Mol Cell Biol. 10, 1754-63

Crow DS, Kurata WE, Lau AF. (1992)
Phosphorylation of connexin43 in cells containing mutant src oncogenes.
Oncogene. 7, 999-1003.

Darrow BJ, Fast VG, Kleber AG, Beyer EC, Saffitz JE. (1996)
Functional and structural assistsment of intercellular communication. Increased conduction velocity and enhanced connexin expression in dibutyryl cAMP-treated cultured cardiac myocytes.
Circ Res. 79, 174-83.

Denker BM, Nigam SK. (1998)
Molecular structure and assembly of the tight junction.
Am J Physiol. 274, 1-9

Deschenes SM, Walcott JL, Wexler TL, Scherer SS, Fischbeck KH. (1997)
Altered trafficking of mutant connexin32.
J Neurosci. 17, 9077-84.

Diez JA, Elvira M, Villalobo A. (1998)
The epidermal growth factor receptor tyrosine kinase phosphorylates connexin32.

Mol Cell Biochem. 187, 201-10.

Filson AJ, Azarnia R, Beyer EC, Loewenstein WR, Brugge JS. (1990)
Tyrosine phosphorylation of a gap junction protein correlates with inhibition of cell-to-cell communication.
Cell Growth Differ. 1, 661-8.

Giepmans BN, Moolenaar WH. (1998)
The gap junction protein connexin43 interacts with the second PDZ domain of the zona occludens-1 protein.
Curr Biol. 8, 931-4.

Giepmans BN, Verlaan I, Moolenaar WH. (2001)
Connexin-43 interactions with ZO-1 and alpha- and beta-tubulin.
Cell Commun Adhes. 8, 219-23.

Gimlich RL, Kumar NM, Gilula NB. (1990)
Differential regulation of the levels of three gap junction mRNAs in Xenopus embryos.
J Cell Biol.110, 597-605.

Ginzberg and Gilula (1979).
Modulation of cell junctions during differentiation of the chiken otocyst sensory epitelium.
Develop Biol. 110-127.

Girod A, Storrie B, Simpson JC, Johannes L, Goud B, Roberts LM, Lord JM, Nilsson T, Pepperkok R. (1999)
Evidence for a COP-I-independent transport route from the Golgi complex to the endoplasmic reticulum.
Nat Cell Biol. 1, 423-30.

Gonzalez-Mariscal L, Betanzos A, Avila-Flores A. (2000)
MAGUK proteins: structure and role in the tight junction.
Semin Cell Dev Biol.11, 315-24.

Guthrie PB, Knappenberger J, Segal M, Bennett MV, Charles AC, Kater SB. (1999)
ATP released from astrocytes mediates glial calcium waves.
J Neurosci. 19, 520-8.

Harigaya Y, Shoji M, Shirao T, Hirai S. (1996)
Disappearance of actin-binding protein, drebrin, from hippocampal synapses in Alzheimer's disease.
J Neurosci Res. 43, 87-92.

Hatanpaa K, Isaacs KR, Shirao T, Brady DR, Rapoport SI. (1999)
Loss of proteins regulating synaptic plasticity in normal aging of the human brain and in Alzheimer disease.

J Neuropathol Exp Neurol. 58, 637-43.

Hayashi K, Ishikawa R, Ye LH, He XL, Takata K, Kohama K, Shirao T. (1996)
Modulatory role of drebrin on the cytoskeleton within dendritic spines in the rat cerebral cortex.
J Neurosci. Nov 16, 7161-70.

Hayashi K, Shirao T. (1999)
Change in the shape of dendritic spines caused by overexpression of drebrin in cultured cortical neurons.
J Neurosci. 19, 3918-25.

Hensley K, Carney JM, Mattson MP, Aksenova M, Harris M, Wu JF, Floyd RA, Butterfield DA. (1994)
A model for beta-amyloid aggregation and neurotoxicity based on free radical generation by the peptide: relevance to Alzheimer disease.
Proc Natl Acad Sci U S A. 91, 3270-4.

Hobman TC, Zhao B, Chan H, Farquhar MG. (1998)
Immunoisolation and characterization of a subdomain of the endoplasmic reticulum that concentrates proteins involved in COPII vesicle biogenesis.
Mol Biol Cell. 9, 1265-78.

Ikeda K, Kaub PA, Asada H, Uyemura K, Toya S, Shirao T. (1996)
Stabilization of adhesion plaques by the expression of drebrin A in fibroblasts.
Brain Res Dev Brain Res. 91, 227-36.

Innocenti B, Parpura V, Haydon PG. (2000)
Imaging extracellular waves of glutamate during calcium signaling in cultured astrocytes.
J Neurosci. 20, 1800-8.

Ishikawa R, Hayashi K, Shirao T, Xue Y, Takagi T, Sasaki Y, Kohama K. (1994)
Drebrin, a development-associated brain protein from rat embryo, causes the dissociation of tropomyosin from actin filaments.
J Biol Chem. 269, 29928-33.

Jongen WM, Fitzgerald DJ, Asamoto M, Piccoli C, Slaga TJ, Gros D, Takeichi M, Yamasaki H. (1991)
Regulation of connexin 43-mediated gap junctional intercellular communication by Ca2+ in mouse epidermal cells is controlled by E-cadherin.
J Cell Biol.114, 545-55.

Kanemitsu MY, Loo LW, Simon S, Lau AF, Eckhart W. (1997)
Tyrosine phosphorylation of connexin 43 by v-Src is mediated by SH2 and SH3 domain interactions.
J Biol Chem. 272, 22824-31.

Kanemitsu MY, Jiang W, Eckhart W. (1998)
Cdc2-mediated phosphorylation of the gap junction protein, connexin43, during mitosis.
Cell Growth Differ. 9, 13-21.

Kasai H, Li YX, Miyashita Y. (1993)
Subcellular distribution of Ca2+ release channels underlying Ca2+ waves and oscillations in exocrine pancreas.
Cell. 74, 669-77.

Keon BH, Jedrzejewski PT, Paul DL, Goodenough DA. (2000)
Isoform specific expression of the neuronal F-actin binding protein, drebrin, in specialized cells of stomach and kidney epithelia.
J Cell Sci. 113, 325-36.

Kim PS, Arvan P. (1998)
Endocrinopathies in the family of endoplasmic reticulum (ER) storage diseases: disorders of protein trafficking and the role of ER molecular
chaperones.
Endocr Rev. 19, 173-202.

Kuehn MJ, Herrmann JM, Schekman R. (1998)
COPII-cargo interactions direct protein sorting into ER-derived transport vesicles.
Nature. 391, 187-90.

Kumar NM, Gilula NB. (1992)
Molecular biology and genetics of gap junction channels.
Semin Cell Biol. 3, 3-16.

Laing JG, Beyer EC. (1995)
The gap junction protein connexin43 is degraded via the ubiquitin proteasome pathway.
J Biol Chem. 270, 26399-403.

Laird, D. W., Puranam, K. L. and Revel, J. P. (1991).
Turnover and phosphorylation dynamics of connexin43 gap junction protein in cultured cardiac myocytes.
Biochem. J. 273, 67 -72.

Laird, D. W., Castillo, M. and Kasprzak, L. (1995).
Gap junction turnover, intracellular trafficking, and phosphorylation of connexin43 in brefeldin A-treated rat mammary tumor cells.
J. Cell Biol. 131,1193 -1203.

Lampe, P. D. (1994).
Analyzing phorbol ester effects on gap junctional communication: a dramatic inhibition of assembly.
J. Cell Biol. 127,1895 -1905.

Lampe PD, Kurata WE, Warn-Cramer BJ, Lau AF. (1998)
Formation of a distinct connexin43 phosphoisoform in mitotic cells is dependent upon p34cdc2 kinase.
J Cell Sci. 111, 833-41.

Lampe PD, TenBroek EM, Burt JM, Kurata WE, Johnson RG, Lau AF. (2000)
Phosphorylation of connexin43 on serine368 by protein kinase C regulates gap junctional communication.
J Cell Biol.149, 1503-12.

Lampe P.D. and Lau A.F. (2000)
Regulation of gap junctions by phosphorylation of connexins.
Arch Biochem Biophys. 384, 205-15.

Lappalainen P, Kessels MM, Cope MJ, Drubin DG. (1998)
The ADF homology (ADF-H) domain: a highly exploited actin-binding module.
Mol Biol Cell. 9, 1951-9.

Larbolette O, Wollscheid B, Schweikert J, Nielsen PJ, Wienands J. (1999)
SH3P7 is a cytoskeleton adapter protein and is coupled to signal transduction from lymphocyte antigen receptors.
Mol Cell Biol. 19, 1539-46.

Larsen and Tung (1978).
Origin and fate of cytoplasmic gap junctional vesicles in rabbit granulosa cell.
Tissue Cell 10, 585-598.

Larsen, W. J., Tung, H. N., Murray, S. A. and Swenson, C. A. (1979).
Evidence for the participation of actin microfilaments and bristle coats in the internalization of gap junction membrane.
J. Cell Biol. 83,576 -587.

Lauf U, Giepmans BN, Lopez P, Braconnot S, Chen SC, Falk MM. (2002)
Dynamic trafficking and delivery of connexons to the plasma membrane and accretion to gap junctions in living cells.
Proc Natl Acad Sci U S A. 99, 10446-51.

Leybaert L, Paemeleire K, Strahonja A, Sanderson MJ. (1998)
Inositol-trisphosphate-dependent intercellular calcium signaling in and between astrocytes and endothelial cells.
Glia. 24, 398-407.

Lim AC, Qi RZ. (2003)
Cyclin-dependent kinases in neural development and degeneration.
J Alzheimers Dis. 5, 329-35.

Lin R, Warn-Cramer BJ,Kurata WE, Lau AF (2001)

v-Src phosphorylation of connexin 43 on Tyr247 and Tyr265 disrupts gap junctional communication.
J Cell Biol. 154, 815-27.

Loo LW, Berestecky JM, Kanemitsu MY, Lau AF. (1995)
pp60src-mediated phosphorylation of connexin 43, a gap junction protein.
J Biol Chem. 270, 12751-61.

Manthey D, Bukauskas F, Lee CG, Kozak CA, Willecke K. (1999)
Molecular cloning and functional expression of the mouse gap junction gene connexin-57 in human HeLa cells.
J Biol Chem. 274, 14716-23.

Martin PE, Blundell G, Ahmad S, Errington RJ, Evans WH. (2001)
Multiple pathways in the trafficking and assembly of connexin 26, 32 and 43 into gap junction intercellular communication channels.
J Cell Sci. 114, 3845-55.

Martinez AD, Hayrapetyan V, Moreno AP, Beyer EC. (2002)
Connexin43 and connexin45 form heteromeric gap junction channels in which individual components determine permeability and regulation.
Circ Res. 90, 1100-7.

Moreno AP. (2002)
Filling more gaps: consequences of heterogeneous remodeling in connexin expression.
J Cardiovasc Electrophysiol. 13, 871-2.

Murray SA, Williams SY, Dillard CY, Narayanan SK, McCauley J. (1997)
Relationship of cytoskeletal filaments to annular gap junction expression in human adrenal cortical tumor cells in culture.
Exp Cell Res. 234, 398-404.

Musil, L. S., Cunningham, B. A., Edelman, G. M. and Goodenough, D. A. (1990).
Differential phosphorylation of the gap junction protein connexin43 in junctional communication-competent and -deficient cell lines.
 J. Cell Biol. 111, 2077 -2088.

Musil LS, Goodenough DA. (1991)
Biochemical analysis of connexin43 intracellular transport, phosphorylation, and assembly into gap junctional plaques.
J Cell Biol. 115, 1357-74.

Musil LS, Goodenough DA. (1993)
Multisubunit assembly of an integral plasma membrane channel protein, gap junction connexin43, occurs after exit from the ER.
Cell. 74, 1065-77.

Musil LS, Le AC, VanSlyke JK, Roberts LM. (2000)
Regulation of connexin degradation as a mechanism to increase gap junction assembly
and function.
J Biol Chem. 275, 25207-15.

Niessen H, Harz H, Bedner P, Kramer K, Willecke K. (2000)
 Selective permeability of different connexin channels to the second messenger inositol
1,4,5-trisphosphate.
J Cell Sci. 113, 1365-72.

Paulson AF, Lampe PD, Meyer RA, TenBroek E, Atkinson MM, Walseth TF, Johnson
RG. (2000)
Cyclic AMP and LDL trigger a rapid enhancement in gap junction assembly through a
stimulation of connexin trafficking.
J Cell Sci. 113, 3037-49.

Peitsch WK, Grund C, Kuhn C, Schnolzer M, Spring H, Schmelz M, Franke WW. (1999)
Drebrin is a widespread actin-associating protein enriched at junctional plaques, defining
a specific microfilament anchorage system in polar epithelial cells.
Eur J Cell Biol. 78, 767-78.

Pepperkok R, Lowe M, Burke B, Kreis TE. (1998)
Three distinct steps in transport of vesicular stomatitis virus glycoprotein from the ER to
the cell surface in vivo with differential sensitivities to GTP gamma S.
J Cell Sci. 111, 1877-88.

Peracchia C, Wang X, Li L, Peracchia LL. (1996)
Inhibition of calmodulin expression prevents low-pH-induced gap junction uncoupling in
Xenopus oocytes.
Pflugers Arch. 431, 379-87.

Peracchia C, Sotkis A, Wang XG, Peracchia LL, Persechini A. (2000)
Calmodulin directly gates gap junction channels.
J Biol Chem. 275, 26220-4.

Phelan P, Starich TA. (2001)
Innexins get into the gap.
Bioessays. 23, 388-96.

De Pina-Benabou MH, Srinivas M, Spray DC, Scemes E. (2001)
Calmodulin kinase pathway mediates the K+-induced increase in Gap junctional
communication between mouse spinal cord astrocytes.
J Neurosci. 21, 6635-43.

Plotkin LI, Bellido T. (2001)
Bisphosphonate-induced, hemichannel-mediated, anti-apoptosis through the Src/ERK
pathway: a gap junction-independent action of

connexin43.
Cell Commun Adhes. 8, 377-82.

Plotkin LI, Manolagas SC, Bellido T. (2002)
Transduction of cell survival signals by connexin-43 hemichannels.
J Biol Chem. 277, 8648-57

Postma FR, Hengeveld T, Alblas J, Giepmans BN, Zondag GC, Jalink K, Moolenaar WH. (1998)
Acute loss of cell-cell communication caused by G protein-coupled receptors: a critical role for c-Src.
J Cell Biol.140, 1199-209.

Qin H, Shao Q, Igdoura SA, Alaoui-Jamali MA, Laird DW. (2003)
Lysosomal and proteasomal degradation play distinct roles in the life cycle of Cx43 in gap junctional intercellular communication-deficient and -competent breast tumor cells.
J Biol Chem. 278, 30005-14.

Robb-Gaspers LD, Thomas AP. (1995)
 Coordination of Ca2+ signaling by intercellular propagation of Ca2+ waves in the intact liver.
J Biol Chem. 270, 8102-7.

Saez JC, Nairn AC, Czernik AJ, Fishman GI, Spray DC, Hertzberg EL. (1997)
Phosphorylation of connexin43 and the regulation of neonatal rat cardiac myocyte gap junctions.
J Mol Cell Cardiol. 29, 2131-45.

Saez JC, Martinez AD, Branes MC, Gonzalez HE. (1998)
Regulation of gap junctions by protein phosphorylation.
Braz J Med Biol Res. 31, 593-600.

Salama NR, Yeung T, Schekman RW. (1993)
The Sec13p complex and reconstitution of vesicle budding from the ER with purified cytosolic proteins.
EMBO J. 12, 4073-82.

Sanderson MJ. (1995)
Intercellular calcium waves mediated by inositol trisphosphate.
Ciba Found Symp. 188, 175-94.

Schekman R, Orci L. (1996)
Coat proteins and vesicle budding.
Science. 271, 1526-33.

Shim KS, Lubec G. (2002)

Drebrin, a dendritic spine protein, is manifold decreased in brains of patients with Alzheimer's disease and Down syndrome.
Neurosci Lett. 324, 209-12.

Shirao T, Sekino Y. (2001)
Clustering and anchoring mechanisms of molecular constituents of postsynaptic scaffolds in dendritic spines.
Neurosci Res. 40, 1-7.

Shirao T, Obata K. (1985)
Two acidic proteins associated with brain development in chick embryo.
J Neurochem. 44, 1210-6.

Shirao T, Hayashi K, Ishikawa R, Isa K, Asada H, Ikeda K, Uyemura K. (1994)
Formation of thick, curving bundles of actin by drebrin A expressed in fibroblasts.
Exp Cell Res. 215, 145-53.

Sohl G, Degen J, Teubner B, Willecke K. (1998)
The murine gap junction gene connexin36 is highly expressed in mouse retina and regulated during brain development.
FEBS Lett. 428, 27-31.

Singh D, Lampe PD. (2003)
Identification of connexin-43 interacting proteins.
Cell Commun Adhes. Jul-Dec; 10(4-6): 215-20.

Sotkis A, Wang XG, Yasumura T, Peracchia LL, Persechini A, Rash JE, Peracchia C. (2001)
Calmodulin colocalizes with connexins and plays a direct role in gap junction channel gating.
Cell Commun Adhes. 8, 277-81.

Spang A. (2002)
ARF1 regulatory factors and COPI vesicle formation.
Curr Opin Cell Biol. 14, 423-7.

Springer S, Spang A, Schekman R. (1999)
A primer on vesicle budding.
Cell. 97, 145-8.

Stevenson BR, Siliciano JD, Mooseker MS, Goodenough DA. (1986)
Identification of ZO-1: a high molecular weight polypeptide associated with the tight junction (zonula occludens) in a variety of epithelia.
J Cell Biol. 103, 755-66.

Stout CE, Costantin JL, Naus CC, Charles AC. (2002)

Intercellular calcium signaling in astrocytes via ATP release through connexin hemichannels.
J Biol Chem. 277, 10482-8.

Stutzmann GE, Caccamo A, LaFerla FM, Parker I. (2004)
Dysregulated IP3 signaling in cortical neurons of knock-in mice expressing an Alzheimer's-linked mutation in presenilin1 results in exaggerated Ca2+ signals and altered membrane excitability.
J Neurosci. 24, 508-13.

Swenson KI, Piwnica-Worms H, McNamee H, Paul DL. (1990)
Tyrosine phosphorylation of the gap junction protein connexin43 is required for the pp60v-src-induced inhibition of communication.
Cell Regul. 1, 989-1002.

Tang BL, Peter F, Krijnse-Locker J, Low SH, Griffiths G, Hong W. (1997)
The mammalian homolog of yeast Sec13p is enriched in the intermediate compartment and is essential for protein transport from the endoplasmic reticulum to
Mol Cell Biol. 17, 256-66.

TenBroek EM, Lampe PD, Solan JL, Reynhout JK, Johnson RG. (2001)
Ser364 of connexin43 and the upregulation of gap junction assembly by cAMP.
J Cell Biol. 155, 1307-18.

Teubner B, Odermatt B, Guldenagel M, Sohl G, Degen J, Bukauskas F, Kronengold J, Verselis VK, Jung YT, Kozak CA, Schilling K, Willecke K. (2001)
Functional expression of the new gap junction gene connexin47 transcribed in mouse brain and spinal cord neurons.
J Neurosci. 21, 1117-26.

Theiss C, Meller K. (2002)
Microinjected anti-actin antibodies decrease gap junctional intercellular commmunication in cultured astrocytes.
Exp Cell Res. 281, 197-204.

Thomas T, Jordan K, Laird DW. (2001)
Role of cytoskeletal elements in the recruitment of Cx43-GFP and Cx26-YFP into gap junctions.
Cell Commun Adhes. 8, 231-6.

Thomas MA, Zosso N, Scerri I, Demaurex N, Chanson M, Staub O. (2003)
A tyrosine-based sorting signal is involved in connexin43 stability and gap junction turnover.
J Cell Sci. 116, 2213-22.

Torok K, Stauffer K, Evans WH. (1997)
Connexin 32 of gap junctions contains two cytoplasmic calmodulin-binding domains.

Biochem J. 326, 479-83.

Toyofuku T, Yabuki M, Otsu K, Kuzuya T, Hori M, Tada M. (1998)
Direct association of the gap junction protein connexin-43 with ZO-1 in cardiac
myocytes.
J Biol Chem. 273, 12725-31.

Toyofuku T, Akamatsu Y, Zhang H, Kuzuya T, Tada M, Hori M. (2001)
c-Src regulates the interaction between connexin-43 and ZO-1 in cardiac myocytes.
J Biol Chem. 276, 1780-8.

Traub O, Look J, Paul D, Willecke K. (1987)
Cyclic adenosine monophosphate stimulates biosynthesis and phosphorylation of the 26
kDa gap junction protein in cultured mouse
hepatocytes.
Eur J Cell Biol. 43, 48-54.

Traub O, Eckert R, Lichtenberg-Frate H, Elfgang C, Bastide B, Scheidtmann KH, Hulser
DF, Willecke K. (1994)
Immunochemical and electrophysiological characterization of murine connexin40 and -
43 in mouse tissues and transfected human cells.
Eur J Cell Biol. 64, 101-12.

Traub O, Look J, Dermietzel R, Brummer F, Hulser D, Willecke K. (1989)
Comparative characterization of the 21-kD and 26-kD gap junction proteins in murine
liver and cultured hepatocytes.
J Cell Biol. 108, 1039-51.

Wang Y, Rose B. (1995)
Clustering of Cx43 cell-to-cell channels into gap junction plaques: regulation by cAMP
and microfilaments.
J Cell Sci. 108, 3501-8.

VanSlyke JK, Deschenes SM, Musil LS. (2000)
Intracellular transport, assembly, and degradation of wild-type and disease-linked mutant
gap junction proteins.
Mol Biol Cell. 11, 1933-46.

VanSlyke JK, Musil LS. (2002)
Dislocation and degradation from the ER are regulated by cytosolic stress.
J Cell Biol. 157, 381-94.

Warn-Cramer BJ, Lampe PD, Kurata WE, Kanemitsu MY, Loo LW, Eckhart W, Lau AF.
(1996)
Characterization of the mitogen-activated protein kinase phosphorylation sites on the
connexin-43 gap junction protein.
J Biol Chem. 271, 3779-86.

Wei C-J, Boja E., Fales HM, Lo CW (2003)
Interaction of the gap junction protein connexin43 whith adherens junction assosiated proteins.
International Gap Junction Conference, abstract book, p144

White TW, Paul DL. (1999)
 Genetic diseases and gene knockouts reveal diverse connexin functions.
Annu Rev Physiol. 61, 283-310.

Willecke K, Eiberger J, Degen J, Eckardt D, Romualdi A, Guldenagel M, Deutsch U, Sohl G. (2002)
Structural and functional diversity of connexin genes in the mouse and human genome.
Biol Chem. 383, 725-37.

Ye ZC, Wyeth MS, Baltan-Tekkok S, Ransom BR. (2003).
Functional hemichannels in astrocytes: a novel mechanism of glutamate release.
J Neurosci. 23, 3588-96.

Yoshihisa T, Barlowe C, Schekman R. (1993)
Requirement for a GTPase-activating protein in vesicle budding from the endoplasmic reticulum.
Science. 259, 1466-8.

Lebenslauf

Angaben zu Person:
Name   Butkevich
Vorname   Eugenia
Geburtsdatum: 19.09.1973
Geburtsort: Omsk, Rußland
Staatsangehörigkeit: weißrussich

1980 – 1988   Allgemeinbildende Schule Minsk, Weißrußland
1988-1991   Medizinische Schule, Minsk
1992 – 1999   Medizinische Universität, Minsk
1999   Diplom im Fach Medizin

1999-2001   Ärztin , Kinderklinikum, Minsk

1995 und 1996   Gaststudentin im Institut für Klinische
                                        Biochemie der Georg-August-Universität
                                        Göttingen.

November 1999 - Februar 2000   Gastwissenschaftlerin in der Abt.
                                        Neurobiologie, Max Plank Institut für
                                        Biophysikalische Chemie, Göttingen.

Februar 2002   Beginn der experimentellen Arbeit zur vorliegenden
                                        Dissertation am Zentrum für Physiologie und
                                        Pathophysiologie der Georg-August-Universität Göttingen

Mai 2004   Fertigstellung der vorliegenden Dissertation